Electron-Deficient Near-Infrared Pt(II) and Pd(II) Benzoporphyrins with Dual Phosphorescence and Unusually Efficient Thermally Activated Delayed Fluorescence: First Demonstration of Simultaneous Oxygen and Temperature Sensing with a Single Emitter

Peter W. Zach,[(a)] Stefan A. Freunberger, [(b)] Ingo Klimant, [(a)] Sergey M. Borisov [(a)]*

(a) Institute of Analytical Chemistry and Food Chemistry, Graz University of Technology, Stremayrgase 9, 8010, Graz, Austria. *E-Mail: sergey.borisov@tugraz.at
(b) Institute for Chemistry and Technology of Materials, Graz University of Technology, Stremayrgase 9, 8010, Graz, Austria.

Keywords: benzoporphyrin, TADF, NIR, upconversion, dual sensor, oxygen, temperature

Abstract

We report a family of Pt and Pd benzoporphyrin dyes with versatile photophysical properties and easy access from cheap and abundant chemicals. Attaching 4 or 8 alkylsulfone groups onto a meso-tetraphenyltetrabenzoporphyrin (TPTBP) macrocylcle renders the dyes highly soluble in organic solvents, photostable, and electron-deficient with the redox potential raised up to 0.65 V versus the parent porphyrin. The new dyes intensively absorb in the blue (Soret band, 440−480 nm) and in the red (Q-band, 620−650 nm) parts of the electromagnetic spectrum and show bright phosphorescence at room-temperature in the NIR with quantum yields up to 30% in solution. The small singlet−triplet energy gap yields unusually efficient thermally activated delayed fluorescence (TADF) at elevated temperatures in solution and in polymeric matrices with quantum yields as high as 27% at 120 °C, which is remarkable for benzoporphyrins. Apart from oxygen sensing, these properties enable unprecedented simultaneous, self-referenced oxygen and temperature sensing with a single indicator dye: whereas oxygen can be determined either via the decay time of phosphorescence or TADF, the temperature is accessed via the ratio of the two emissions. Moreover, the dyes are efficient sensitizers for triplet−triplet annihilation (TTA)- based upconversion making possible longer sensitization wavelength than the conventional benzoporphyrin complexes. The Ptocta-sulfone dye also features interesting semireversible transformation in basic media, which generates new NIR absorbing species.

1. Introduction

Porphyrins play a central role in many biological processes pivotal to life and are probably the most important functional pigments found in nature.[1][2]–[4] They are square, planar 18 π-

electron aromatic macrocycles comprising four pyrroles and four methine carbons. A rich variety of substituents in the macrocycle and of the central transition metal cation endows them with diverse functionality in nature and in human-designed applications. Platinum(II) and palladium(II) porphyrins are very popular luminophores due to their strong room temperature phosphorescence and large Stokes shifts.[5] Efficient quenching of phosphorescence by molecular oxygen enables optical oxygen sensors.[6] Phosphorescent dyes absorbing in the red and emitting in the near-infrared (NIR) optical window (700-950 nm) are particularly promising for various medical and therapeutic applications due to high tissue transparency and low autofluorescence.[7] For instance, they proved to be excellent tools for microscopic *in vivo* imaging of tissue oxygenation, e.g., of tumors, blood vessels, brain slices etc. Recently, NIR phosphorescent dyes were applied as indicators in a system combining continuous subcutaneous glucose monitoring and insulin infusion.

Similarly to other chemosensors, the response of optical oxygen sensors is temperature-dependent and has to be compensated for. This can be done via an external probe (e.g., a resistance thermometer) or with an optical temperature probe [8], which can be combined with the oxygen probe in a dual sensor.[9]–[14] While the first method lacks spatial resolution, dual sensors are complex in design and often suffer from undesirable effects including optical cross-talk and chemical interferences between oxygen and temperature probes. Although numerous systems for simultaneous sensing of oxygen and temperature have been reported [8], to the best of our knowledge there are no systems based on a single probe.

Phosphorescent dyes are also particularly useful as sensitizers for upconversion systems based on triplet-triplet annihilation (TTA).[15],[16] TTA upconversion overcomes the drawbacks of other upconversion techniques such as lanthanide upconversion and multi-photon excitation. It is observed at low excitation power densities (typical for, e.g., solar light) [17] and enables for varying the excitation and emission wavelength by tuning triplet sensitizer and triplet acceptor.[18] Recent research was focused on developing highly photostable and soluble triplet sensitizers in the red.[19]–[22] Sensitizers with a small singlet-triplet energy gap are advantageous since they enable longer sensitization wavelengths and are compatible with annihilators with relatively high triplet state energy.

The most promising way to achieve a bathochromic shift of the absorption and the emission bands of porphyrinoids is the extension of the π-conjugated system of the porphyrin core through fusion of various aromatic moieties at the β-pyrrole positions [23]–[25] leading, for example, to tetrabenzoporphyrins (TBP) or tetranaphthaloporphyrins (TNP) [26]. These complexes have only moderate solubility due to strong tendency to π-π-stacking [27], but the solubility can be improved by introducing phenyl rings at the meso-position of the porphyrin core and other bulky substituents such as tert-butyl groups. [28] Photostability is another

parameter which may need improvement; it is, for instance, particularly poor for naphthoporphyrins bearing no electron-withdrawing substituents.[29] Zems et al. have recently reported the synthesis of a highly soluble platinum(II) porphyrin with excellent solubility and very high photostability.[4] Nevertheless, the multi-step synthesis (10 steps) and poor availability and high cost of some intermediates (such as tert-butyl isocyano acetate) limit practical applicability of this interesting compound.

Herein we present electron-deficient highly soluble and photostable platinum(II) and palladium(II) benzoporphyrins bearing alkylsulfone groups that are accessible via a convenient and simple synthetic strategy with only four steps from cheap and abundant precursors. All new dyes feature a smaller singlet-triplet energy gap compared to state-of-the-art benzoporphyrins. This gives rise to unusually efficient TADF at elevated temperatures (particularly for Pd-O-S and Pd-T-I). We will demonstrate their applicability for simultaneous measurement of oxygen and temperature with a single probe, which is so far unique in literature. We also show that the new dyes are very promising for TTA-based upconversion since they can harvest more energy in the red part of the spectrum and transfer it to a variety of annihilators.

2. Experimental Section

Materials

(3aR,7aS)-3a,4,7,7a-tetrahydroisobenzofuran-1,3-dione, 2-ethylhexane-1-thiol, potassium t-butoxide, 2-ethylhexylamine, N-chlorosuccinimide, thiophenol, potassium carbonate, tetraoctylammonium hydroxide solution (20% in methanol), trifluoroacetic acid, chlorotrimethylsilane and water-free dichloromethane (DCM) were purchased from Sigma Aldrich. Meta-chloroperoxybenzoic acid (m-CPBA), 1,2,4-trimethylbenzene (TMB), aluminum oxide (neutral, 50-200 µm; Al_2O_3), Polystyrene-co-acrylontrile (PSAN; 25 wt% acrylonitrile; Mw = 165,000 $g \cdot mol^{-1}$) and polystyrene (PS; Mw = 260,000 $g \cdot mol^{-1}$) were obtained from Acros Organics. 1,8-diaza-7-bicyclo[5.4.0]undecene (DBU), perylene and dimethylacetamide (DMA) were from Fluka. Ethyl 2-isocyanoacetate, 2-(4-fluorophenyl)acetic acid and Solvent Green 5 (diisobutyl 3,9-perylenedicarboxylate) were purchased from ABCR. Dry dimethylformamide (DMF), dry hexane silica gel 60 and zinc oxide were obtained from Merck. Zinc-4-fluorophenylacetate was obtained as a white precipitate in an exchange reaction between zinc acetate and 2-(4-fluorophenyl)acetic acid. Sodium hydrogen carbonate, sodium sulfate, sodium chloride and sodium carbonate were from VWR. 4,5-dichlorophthalonitrile and boron trifluoride etherate, Indocyanine green were purchased from TCI. Ultrafine TiO_2 P170 was obtained from Kemira. Silicone E4 was purchased from Wacker chemicals.

Solvent Green 5 and N,N′-bis-(2,6-diisopropylphenyl)-perylene-3,4,9,10-tetracarboxylic acid diimide (Lumogen F Orange) were obtained from Kremer Pigmente GmbH and Co. KG (Aichstetten, Germany). Cyclohexane (CH), ethyl acetate (EE), n-hexane, dry tetrahydrofuran (THF) as well as toluene and chloroform in HPLC-grade were obtained from Roth. Methanol (MeOH) was from Baker, whereas ethanol (EtOH) was from Australco. Toluene and dichloromethane (DCM) were obtained from Fisher Chemicals. Nitrogen, argon (both 99.999% purity) was purchased from Air Liquide, oxygen (99.999% purity) and oxygen (2%) in nitrogen (test gas) from Linde Gas. Poly(ethylene terephthalate) (PET) support Melinex 505 was purchased from Pütz.

Platinum chloride and palladium chloride for the synthesis of the respective precursor were obtained from ChemPur. The precursors $Pt(C_6H_5CN)_2Cl_2$ as well as the $Pd(C_6H_5CN)_2Cl_2$ were obtained by stirring $PtCl_2$ or $PdCl_2$ in boiling benzonitrile for one hour and precipitating the resulted product with hexane. The formed yellow product was filtered, washed with hexane, and dried at 60 °C in the vacuum oven. The reference compounds platinum(II) and palladium(II) complexes of meso-tetraphenyltetrabenzoporpyhrin (Pt-TPTBP and Pd-TPTBP, respectively) were prepared according to a literature procedure. [30]

Synthesis

Nomenclature

Intermediates and final products are abbreviated with the nomenclature Metal-(number of sulfones)-ring. For the number of sulfones O stands for the octa-sulfone and T for the tetra-sulfone. For the ring T stands for the thio…, S for the …, I for the …

4,5-bis((2-ethylhexyl)thio)phthalonitrile

The reaction was conducted according to the literature procedure [31]. 4,5-dichlorophthalonitrile (9.00 g, 45.68 mmol, 1.00 eq) was first dissolved in 100 mL dimethylacetamide (DMA) in a 2-neck round bottom flask and the solution was degassed in argon counterflow for 10 minutes. Then ground, dry K_2CO_3 (18.00 g, 130.2 mmol, 2.85 eq) was added and the solution was again degassed for further 10 minutes. 2-ethylhexane-1-thiol (14.71 g, 100.6 mmol, 2.20 eq, ρ=0.8430 g/mL) was added and the resulting reaction mixture was heated to 90 °C for 8 hours (vigorous stirring). Afterwards, the reaction mixture was poured onto dest. H_2O and extracted with DCM (3 times). The organic fraction was washed with dest. H_2O (6 × 100 mL) to remove dimethylacetamide, dried over Na_2SO_4, before the solvent was finally evaporated in vacuo to afford the product as yellow oil. Yield: 14.85 g, 78 %.

^{1}H NMR (300 MHz, Chloroform-*d*) δ 7.41 (s, 2H), 2.97 (d, *J* = 6.2 Hz, 4H), 1.71 (p, *J* = 6.2 Hz, 2H), 1.58-1.40 (m, 8H), 1.36-1.26 (m, 8H), 0.94-0.84 (m, 12H).

*Zinc(II) meso-tetra(4-fluorophenyl)tetra(4,5-bis((2-ethylhexyl)thio)benzo-porphyrin (**Zn-O-T**)*

4,5-bis((2-ethylhexyl)thio)phthalonitrile (12.94 g, 31.05 mmol, 4.00 eq), 2-(4-fluorophenyl)acetic acid (11.96 g, 77.59 mmol, 10.00 eq), zinc-4-fluorophenylacetate (2.90 g, 7.76 mmol, 1.00 eq) were mixed together and homogenized with a ceramic pestle in a mortar. Approximately 700 mg of the mixture were weighed in 4 mL glass vials equipped with a stirring bar. The vials were sealed with a metal cap and put on a 160 °C heating block and then heated up to 280 °C. After reaching 280 °C the stirrer was started and the reaction mixture was kept at this temperature for 40 minutes. Then the vials were removed from the heating source and cooled down. Afterwards the vials were smashed with a hammer and the reaction products were dissolved in 800 mL acetone in an ultrasonic bath. The pieces of glass were separated via filtration and the solvent was removed under reduced pressure. The residue was re-dissolved in 800 mL cyclohexane/n-hexane (2:1) and washed with methanol (6 × 300 mL). The impurities were removed via column chromatography (silica-gel, CH:DCM, 2:1) and the product dried in the vacuum oven at 60 °C. Yield: 0.92 g, 6%. This intermediate was used in further step without further purification.

UV-Vis: $\lambda_{max}/\varepsilon$ (nm, $M^{-1}cm^{-1}$) in toluene: 478/ 347.000, 625/ 19.000, 678/ 115.000

MALDI: m/z: [M^+]; $C_{124}H_{160}F_4N_4S_8Zn$, calc.: 2103.966; found: 2103.964

*Meso-tetra(4-fluorophenyl)tetra(4,5-bis((2-ethylhexyl)thio)benzoporphyrin (**H_2-O-T**)*

Zn-O-T (430 mg, 204.3 µmol) was dissolved in 200 mL DCM and 50 mL of 4 M HCl were added. The resulting protonated ligand could be determined via absorption spectra ($\lambda_{max}/\varepsilon$ (nm, $M^{-1}cm^{-1}$) in toluene: 423/ 0.090, 524/ 1.00, 662/ 0.076, 721/ 0.087). The organic phase was washed twice with and then with saturated $NaHCO_3$-solution until only neutral ligand was observed in the absorption spectra. Finally the organic layer was once more washed with dest. H_2O, dried over Na_2SO_4 and the solvent was removed under reduced pressure. Yield: 380 mg, 91%. The product was introduced in the next step without further purification due to its high tendency to oxidation.

UV-Vis: $\lambda_{max}/\varepsilon$ (nm, $M^{-1}cm^{-1}$) in toluene: 475/ 155.000, 490/ 154.000, 614/ 12.000, 668/ 50.000, 717/ 17.000

MALDI: m/z: [M^+]; $C_{124}H_{162}F_4N_4S_8$, calc.: 2040.053; found: 2040.038

*Meso-tetra(4-fluorophenyl)tetra(4,5-bis((2-ethylhexyl)sulfoneyl)benzoporphyrin (**H_2-O-S**)*

H_2-O-T (245 mg, 120 µmol, 1.00 eq) was dissolved in 30 mL DCM in a round bottom flask and m-CPBA (518 mg, 3 mmol, 25.00 eq) was added slowly to the stirring solution using a plastic spatula. The solution was shielded from light and the reaction progress monitored via absorption spectra and TLC. After complete conversion, the reaction mixture was quenched with saturated $NaHCO_3$-solution, extracted with DCM (3 × 60 mL) and dried over Na_2SO_4. The

solvent was removed under reduced pressure. Finally, the crude product was purified via column chromatography (silica-gel, CH:EE, 9:1) to yield **H_2-O-S** as dark green solid. Yield: 165 mg, 60 %.

UV-Vis. λ_{max}(nm)/relative intensity in toluene: 488/ 1.00, 599/ 0.061, 638/ 0.088, 709/ 0.011

^{1}H NMR (300 MHz, Methylene Chloride-d_2) δ 8.48 – 8.20 (m, 16H), 7.89 – 7.68 (m, 8H), 3.69 – 3.43 (m, 16H), 1.95 (dq, J = 12.0, 6.5 Hz, 8H), 1.55 – 1.36 (m, 33H), 1.33 – 1.14 (m, 35H), 0.88 – 0.78 (m, 50H).

^{13}C NMR (76 MHz, CD_2Cl_2) δ 167.12, 163.77, 138.14, 135.91, 135.79, 135.76, 118.40, 117.87, 117.59, 60.59, 35.03, 32.96, 28.50, 26.32, 14.17, 10.39.

MALDI: m/z: [M^+]; $C_{124}H_{162}F_4N_4O_{16}S_8$, calc.: 2296.973; found: 2296.988

*Pt(II) meso-tetra(4-fluorophenyl)tetra(4,5-bis((2-ethylhexyl)sulfoneyl)benzo-porphyrin (**Pt-O-S**)*

H_2-O-S (50 mg, 22.77 µmol, 1.00 eq) was dissolved in TMB (15 mL) in a 2-neck-round bottom flask and heated to 175 °C while bubbling N_2 through the reaction mixture. Then $Pt(C_6H_5CN)_2Cl_2$ (103 mg, 217.7 µmol, 10 eq) was added slowly in small portions (5 × 2 eq pre-dissolved in hot TMB) from a pre-heated addition funnel (100 °C) over a period of 3 hours. The reaction progress was monitored via absorption spectra. After completion the reaction mixture was cooled down to room temperature, the by-products were removed via filtration over a short pad of silica-gel. The solvent was removed under reduced pressure at 80 °C. The crude product was further purified via column chromatography (silica-gel, CH:EE, 9:1). The product containing fractions were determined via absorption spectrum and the solvent was removed under reduced pressure. Yield: 165 mg, 60 %.

UV-Vis: $\lambda_{max}/\varepsilon$ (nm, $M^{-1}cm^{-1}$) in toluene: 455/ 370.000, 572/ 25.000, 621/ 229.000

^{1}H NMR (500 MHz, CD_2Cl_2) δ 8.22 (s, 16H), 7.76 (dq, *J* = 8.4, 2.8 Hz, 8H), 3.62 – 3.49 (m, 16H), 1.95 (dq, *J* = 11.6, 5.8 Hz, 8H), 1.49 (q, *J* = 7.1 Hz, 16H), 1.45 – 1.34 (m, 20H), 1.33 – 1.17 (m, 36H), 0.92 – 0.78 (m, 47H)

^{13}C NMR (126 MHz, CD_2Cl_2) δ 166.07, 164.05, 139.24, 137.33, 136.67, 134.55, 134.49, 129.97, 120.74, 117.81, 117.63, 60.21, 34.61, 32.56, 28.09, 25.93, 22.69, 13.73, 9.97.

MALDI: m/z: [M^+]; $C_{124}H_{160}F_4N_4O_{16}S_8Pt$, calc.: 2489.9211; found: 2489.9229

*Pd(II) meso-tetra(4-fluorophenyl)tetra(4,5-bis((2-ethylhexyl)sulfoneyl)benzo-porphyrin (**Pd-O-S**)*

H_2-O-S (45 mg, 19.59 µmol, 1.00 eq) was dissolved in toluene (10 mL) in a 2-neck-round bottom flask and heated to 110 °C, while bubbling N_2 through the reaction mixture. Then $Pd(C_6H_5CN)_2Cl_2$ (9 mg, 23.51 µmol, 1.2 eq) was added slowly in small portions (4 × 0.3 eq pre-dissolved in hot toluene) from a pre-heated addition funnel (100 °C) over a period of 2 hours.

The reaction progress was monitored via absorption spectra. After completion the reaction mixture was cooled down to room temperature, the by-products were removed via filtration over a short pad of silica-gel. The solvent was removed under reduced pressure at 60 °C. The crude product was further purified via column chromatography (silica-gel, CH:EE, 4:1). The product containing fractions were determined via absorption spectrum and the solvent was removed under reduced pressure. Yield: 36 mg, 77 %.

UV-Vis. $\lambda_{max}/\varepsilon$ (nm, $M^{-1}cm^{-1}$) in toluene: 422/ 36.000, 438/ 58.000, 469/ 446.000, 588/ 23.000 636/ 195.000

^{1}H NMR (300 MHz, CD_2Cl_2) δ 8.29 – 8.16 (m, 16H), 7.75 (t, *J* = 8.4 Hz, 8H), 3.69 – 3.37 (m, 15H), 2.03 – 1.85 (m, 8H), 1.51 – 1.44 (m, 16H), 1.43 – 1.33 (m, 24H), 1.32 – 1.12 (m, 34H), 0.93 – 0.74 (m, 47H).

^{13}C NMR (76 MHz, CD_2Cl_2) δ 167.11, 163.76, 139.93, 139.05, 137.53, 135.36, 135.32, 135.23, 135.13, 130.32, 120.62, 118.12, 117.83, 60.59, 35.00, 32.95, 28.49, 26.31, 23.12, 14.15, 10.38.

MALDI: m/z: [M^+]; $C_{124}H_{160}F_4N_4O_{16}S_8Pd$, calc.: 2400.8601; found: 2400.6062

4-((2-ethylhexyl)thio)phthalonitrile

4-nitrophthalonitrile (8.50 g, 49.10 mmol, 1.00 eq) was first dissolved in 110 mL dimethylacetamide (DMA) in a 2-neck round bottom flask and the solution was degassed in argon-counterflow for 10 minutes. Then ground, dry K_2CO_3 (19.34 g, 139.92 mmol, 2.85 eq) was added and the solution was degassed again for further 10 minutes. Then 2-ethylhexane-1-thiol (10.77 g, 73.64 mmol, 1.5 eq, ρ=0.8430 g/mL) was added and the resulting reaction mixture heated to 90 °C for 15 hours (vigorous stirring). Afterwards the reaction mixture was poured onto dest. H_2O and extracted with DCM (6 times). The organic fraction was washed with dest. H_2O (6 x 100 mL) to remove DMA, then dried over Na_2SO_4 before the solvent was finally evaporated under educed pressure. Finally, the crude product was purified via column chromatography on silica gel to afford the product as yellow oil. Yield: 12.82 g, 96 %.

^{1}H NMR (300 MHz, $CDCl_3$) δ 7.63 (d, J = 8.3 Hz, 1H), 7.55 (d, J = 1.9 Hz, 1H), 7.49 (dd, J = 8.4, 2.0 Hz, 1H), 2.97 (d, J = 6.2 Hz, 2H), 1.66 (p, J = 6.2 Hz, 1H), 1.55- 1.37 (m, 4H), 1.31 (dh, J = 7.3, 3.7 Hz, 4H), 0.99-0.84 (m, 6H).

*Zinc(II) meso-tetra(4-fluorophenyl)tetra(4- ((2-ethylhexyl)thio)benzo-porphyrin (**Zn-T-T**)*

The synthesis and purification were performed analogously to **Zn-O-T** but 18.00 g (66.08 mmol, 4.00 eq) of 4-((2-ethylhexyl)thio)phthalonitrile, 25.46 g (165.19 mmol, 10.00 eq) of 2-(4-fluorophenyl)acetic acid and 6.14 (16.52 mmol, 1.00 eq) of zinc 4-fluorophenylacetate were used instead. This intermediate was used in further step without further purification. Yield: 0.98 g, 4%.

UV-Vis. λ_{max}(nm)/relative intensity in toluene: 470/ 1.00, 615/ 0.058, 666/ 0.312
MALDI: m/z: [M^+]; $C_{92}H_{96}F_4N_4S_4Zn$, calc.: 1526.5754; found: 1526.6571

*Meso-tetra(4-fluorophenyl)tetra(4-((2-ethylhexyl)thio)benzoporphyrin (**H_2-T-T**)*
The demetalation was performed analogously to **H_2-O-T** but with 512 mg (335.21 µmol, 1.00 eq) of **Zn-T-T**. The product was introduced in the next step without further purification due to its high tendency to oxidation. Yield: 485 mg, 97%
λ_{max}(nm)/relative intensity in toluene: 474/ 1.00, 599/ 0.202, 649/ 0.173, 707/ 0.059
MALDI: m/z: [M^+]; $C_{92}H_{98}F_4N_4S_4$, calc.: 1463.6642; found: 1463.9174

*Meso-tetra(4-fluorophenyl)tetra(4-((2-ethylhexyl)sulfoneyl)benzoporphyrin (**H_2-T-S**)*
The synthesis and purification were performed analogously to **H_2-O-S** but 450 mg (307.36 µmol, 1.00 eq) of **H_2-T-T** was dissolved in 30 mL DCM in a round bottom flask and m-CPBA (663 mg, 3.84 mmol, 12.50 eq) were used instead. Yield: 230 mg, 47 %.
UV-Vis. λ_{max}(nm)/relative intensity in toluene: 475/ 1.00, 593/ 0.054, 631/ 0.109
^{1}H NMR (300 MHz, Methylene Chloride-d_2) δ 8.48 – 8.20 (m, J = 7.8, 6.7 Hz, 8H), 7.87 – 7.54 (m, 29H), 3.13 – 2.91 (m, 10H), 1.93 – 1.81 (m, 4H), 1.52 – 1.31 (m, 24H), 1.33 – 1.10 (m, 28H), 0.94 – 0.72 (m, 40H).
^{13}C NMR (76 MHz, CD_2Cl_2) δ 166.40, 163.08, 137.17, 136.40, 136.32, 125.31, 117.29, 117.01, 60.14, 34.86, 34.62, 32.87, 32.72, 28.53, 26.25, 26.08, 23.09, 14.18, 10.36.
MALDI: m/z: [M^+]; $C_{92}H_{98}F_4N_4O_8S_4$, calc.: 1591.6235; found: 1591.6461

*Pt(II) meso-tetra(4-fluorophenyl)tetra(4-((2-ethylhexyl)sulfoneyl)benzo-porphyrin (**Pt-T-S**)*
The synthesis and purification were performed analogously to **Pt-O-S** but 55 mg (34.55 µmol, 1.00 eq) of **H_2-T-S** and 20 mg (41.46 µmol, 1.2 eq) of $Pt(C_6H_5CN)_2Cl_2$ (4 x 0.3 eq) were used instead. Yield: 40 mg, 65 %.
UV-Vis. $\lambda_{max}/\varepsilon$ (nm, $M^{-1}cm^{-1}$) in toluene: 441/ 255.000, 570/ 18.000, 619/ 145.000
^{1}H NMR (500 MHz, CD_2Cl_2) δ 8.31 – 8.19 (m, 8H), 7.88 – 7.78 (m, 4H), 7.78 – 7.66 (m, 10H), 7.63 (dd, *J* = 4.3, 1.6 Hz, 2H), 7.41 (dd, *J* = 8.6, 3.3 Hz, 2H), 7.30 (dd, *J* = 8.6, 3.4 Hz, 2H), 3.02 (q, *J* = 5.6 Hz, 8H), 1.88 (dh, *J* = 12.6, 6.2 Hz, 4H), 1.48 (p, *J* = 6.4, 5.9 Hz, 8H), 1.44 – 1.33 (m, 8H), 1.29 – 1.14 (m, 17H), 0.88 – 0.80 (m, 24H).
^{13}C NMR (76 MHz, CD_2Cl_2) δ 166.44, 163.11, 140.72, 140.60, 138.11, 137.41, 136.64, 136.59, 135.53, 135.42, 125.13, 117.70, 117.42, 60.14, 34.86, 32.86, 28.53, 26.25, 23.09, 14.17, 10.37.
MALDI: m/z: [M^+]; $C_{92}H_{96}F_4N_4O_8S_4Pt$, calc.: 1784.8007; found: 1784.6431

*Pd(II) meso-tetra(4-fluorophenyl)tetra(4-((2-ethylhexyl)sulfoneyl)benzo-porphyrin (**Pd-T-S**)*

The synthesis and purification were performed analogously to **Pd-O-S** but 60 mg (37.7 µmol, 1.00 eq) of **H_2-T-S** and 17 mg (45.2 µmol, 1.2 eq) of $Pd(C_6H_5CN)_2Cl_2$ were used instead. Yield: 41 mg, 64 %.

UV-Vis. $\lambda_{max}/\varepsilon$ (nm, $M^{-1}cm^{-1}$) in toluene: 426/ 53.000, 454/ 328.000, 585/ 17.000, 633/ 125.000

^{1}H NMR (300 MHz, CD_2Cl_2) δ 8.37 – 8.15 (m, 8H), 7.89 – 7.61 (m, 16H), 7.43 (dd, *J* = 8.6, 2.0 Hz, 2H), 7.32 (dd, *J* = 8.7, 2.0 Hz, 2H), 3.10 – 2.93 (m, 8H), 1.87 (p, *J* = 5.3 Hz, 4H), 1.51 – 1.35 (m, 13H), 1.30 – 1.12 (m, 20H), 0.93 – 0.76 (m, 26H).

^{13}C NMR (76 MHz, CD_2Cl_2) δ 166.42, 163.09, 141.02, 140.88, 139.25, 138.47, 138.03, 137.79, 136.94, 136.89, 135.75, 135.64, 125.18, 125.01, 124.73, 117.57, 117.29, 60.16, 34.86, 32.86, 28.53, 26.26, 23.09, 14.17, 10.37.

MALDI: m/z: [M^+]; $C_{92}H_{96}F_4N_4O_8S_4Pd$, calc.: 1694.3896 ; found: 1694.5107

*Pt(II) mesotetraphenyltetra2-(2-ethylhexyl)hexahydro-1H-isoindole-1,3(2H)-dione-porphyrin (**Pt-TPThIIP**)*

The synthesis and purification were performed analogously to **Pt-O-S** but 100 mg (64.26 µmol, 1.00 eq) of **H_2-TPThIIP** (obtained according to a modified literature procedure, see supporting information) and 303 mg (642.6 µmol, 10 eq) of $Pt(C_6H_5CN)_2Cl_2$ 5 × 2 eq) were used instead. Yield: 56 mg, 50 %.

UV-Vis. λ_{max}(nm)/relative intensity in toluene: 416/ 1.00, 525/ 0.106, 555/ 0.053

*Pt(II) meso-tetraphenyltetrabenzo-1-(2-ethylhexyl)pyrrolidine-2,5-dione-porphyrin (**Pt-T-I**)*

Pt-TPThIIP (56 mg, 32.02 µmol, 1.00 eq) was dissolved in toluene (8 ml) in a Schlenk flask under a flow of argon and heated to 110 °C. Then DDQ (109 mg, 480.2 µmol, 15 eq) was added in argon counterflow and the reaction mixture was stirred for 4 hours. The reaction was shielded from light and the reaction progress monitored via absorption spectra and TLC. After complete conversion, the reaction mixture was quenched with Na_2SO_3-solution(10%), extracted with DCM (3 × 25 mL) and dried over Na_2SO_4. The solvent was removed under reduced pressure. Finally, the crude product was purified via column chromatography (silica gel, CH:EE, 8:1) The product containing fractions were determined via absorption spectrum and dried in the vacuum oven at 60 °C. Yield: 18 mg, 32 %.

UV-Vis. $\lambda_{max}/\varepsilon$ (nm, $M^{-1}cm^{-1}$) in toluene: 463/ 283.000, 582/ 21.000, 633/ 184.000

^{1}H NMR (300 MHz, CD_2Cl_2) δ 8.29 (d, *J* = 7.1 Hz, 8H), 8.21 (t, *J* = 7.5 Hz, 4H), 8.06 (t, *J* = 7.5 Hz, 8H), 7.43 (s, 8H), 3.52 (d, *J* = 7.1 Hz, 8H), 1.85 – 1.70 (m, 4H), 1.37 – 1.20 (m, 41H), 0.92 – 0.81 (m, 28H).

^{13}C NMR (76 MHz, CD_2Cl_2) δ 168.62, 141.39, 140.45, 137.62, 134.06, 131.20, 130.70, 129.49, 121.57, 120.01, 54.00, 42.54, 39.05, 31.19, 29.22, 24.48, 23.54, 14.40, 10.79.

MALDI: m/z: [M^+]; $C_{100}H_{96}N_8O_8Pt$, calc.: 1732.7025; found: 1732.6790

*Pd(II) tetraphenyltetra2-(2-ethylhexyl)hexahydro-1H-isoindole-1,3(2H)-dione-porphyrin (**Pd-TPThIIP**)*

The synthesis and purification were performed analogously to **Pd-O-S** but 95 mg (61.05 µmol, 1.00 eq) of **H_2-TPThIIP** and 94 mg (244.2 µmol, 4 eq) of $Pd(C_6H_5CN)_2Cl_2$ (4 x 1 eq) were used instead. Yield: 60 mg, 59 %.

λ_{max}(nm)/relative intensity in toluene: 431/ 1.00, 539/ 0.090, 572/ 0.005

*Pd(II) meso-tetraphenyltetrabenzo-1-(2-ethylhexyl)pyrrolidine-2,5-dione-porphyrin (**Pd-T-I**)*

The synthesis and purification were performed analogously to **Pt-T-I** but 60 mg (36.13 µmol, 1.00 eq) of **Pd-TPThIIP** and 123 mg (542.0 µmol, 15 eq) of DDQ were used instead. Yield: 24 mg, 40 %.

UV-Vis. $\lambda_{max}/\varepsilon$ (nm, $M^{-1}cm^{-1}$) in toluene: 478/ 390.000, 597/ 22.000, 648/ 179.000

^{1}H NMR (300 MHz, CD_2Cl_2) δ 8.29 (d, 8H), 8.21 (t, *J* = 7.5 Hz, 4H), 8.06 (t, *J* = 7.5 Hz, 8H), 3.52 (d, *J* = 7.1 Hz, 8H), 1.85 – 1.71 (m, 4H), 1.39 – 1.16 (m, 38H), 0.97 – 0.78 (m, 27H).

^{13}C NMR (76 MHz, CD_2Cl_2) δ 167.27, 140.05, 139.10, 136.27, 132.71, 129.85, 129.35, 128.15, 120.23, 118.67, 41.20, 37.70, 29.84, 27.87, 23.14, 22.20, 13.05, 9.45.

MALDI: m/z: [M^+]; $C_{100}H_{96}N_8O_8Pd$, calc.: 1642.6415; found: 1642.7184

Preparation of Sensor Films

Sensor films of various thicknesses (wet film thickness of 25 or 75 µm) were prepared by coating the dye “cocktails” on a dust-free PET support using a 25 mm-wide Gardner coating knife (Pompano Beach, United States). The polystyrene (as well as PSAN)-based “cocktails” typically contained 1 - 2.5 wt% dye (in respect of the polymer) and 8-10 wt% of polymer dissolved in chloroform (HPLC-grade). After the coating, the sensor films were dried for 24 hours at 60 °C to ensure complete removal of solvent.

For the TADF measurements the polystyrene or PSAN-based dye “cocktails” in $CHCl_3$ ($1.12 \cdot 10^{-6}$ M of the dye) were knife coated on a glass slide (thickness of the wet film: 12.5 µm) which was silanised with chlorotrimethylsilane prior to use. The sensors were dried in the oven at 60 °C for 12 hours.

Measurements

NMR and Mass Spectra

^{1}H and ^{13}C NMR were recorded on a 300 MHz instrument (Bruker AVANCE III) or 500 MHz from Varian. In all ^{1}H and ^{13}C spectra, the residual signal of the deuterated solvent was used as an internal standard to reference the chemical shifts δ. Data analysis was done with the MestraNova NMR software. High resolution mass spectra were recorded using a Micromass TofSpec 2E as positive reflector on a Bruker Ultraflex Extreme MALDI-TOF/TOF spectrometer. The mass spectra were analyzed with the FlexAnalysis 3.0 software (Bruker Daltonics).

Absorption and Luminescence Spectra, Quantum Yield and Decay time measurements

The absorption spectra were recorded on a Varian CARY 50 UV-Vis spectrophotometer (Palo Alto, United States). Molar absorption coefficients were determined in toluene (HPLC-grade) as an average of three independent measurements. Luminescence spectra were recorded on a FluoroLog® 3 spectrofluorometer from Horiba Scientific equipped with a NIR-sensitive R2658 photomultiplier from Hamamatsu (300-1050 nm). Relative quantum yields were determined according to Crosby and Demas [32] using Pt-TPTBP (φ=0.51) [33] and Pd-TPTBP (φ=0.21 [33]) in toluene as referenceswith dye concentrations between 2 and $4 \cdot 10^{-6}$ $mol \cdot l^{-1}$. All dye solutions were deoxygenated in a screw-cap cuvette (Hellma; Müllheim, Germany) by bubbling argon through the solution for 10 minutes. For the TADF studies in solution the temperature of the cuvette was adjusted with a Peltier-element cuvette adaptor from Varian. Absolute quantum yields of the dyes embedded in polystyrene were measured using a Quanta-ϕ integrating sphere from Horiba. To ensure deoxygenated conditions within the experiment, the stamped out pieces of dye-coated PET support were placed in a 5% Na_2SO_3 solution containing traces of $CoCl_2$ as a catalyst. Phosphorescence decay times in solution were determined in the frequency domain with a Firesting oxygen meter from PyroScience (modulation frequencies of 4 kHz and 500 Hz for Pt(II) and Pd(II) complexes, respectively).

TADF Measurements of Immobilized Dyes

The glass slides were placed in a home-made flow-through cell through which the gas was passed with a pressure of 1 bar. The gas was heated to the respective temperature in a home-made oven. The exact temperature in the chamber of the flow-through cell was determined using a Pt-100 temperature sensor connected to a Firesting oxygen meter from PyroScience. Excitation was either performed with the 450 W xenon lamp (steady state measurements) or with SpectraLED 460 nm (decay time measurements) from Horiba.

Photostability Tests

Dye solutions in toluene (HPLC-grade) were placed in a screw-cap cuvette (Hellma) and illuminated with a high-power LED (λ_{max} 617 nm, LT-2033, LED-TECH) at the 28 V and 550 mA. The light of the LED-array was focused onto the glass cuvette using a lens from Edmund

optics. The photon flux was 18.000 µmol s^{-1} m^{-2} µA (irradiance 350 mW·cm^{-2}) as determined with a Li-250A light meter from Li-COR. For measurements at air saturation the cuvette was unsealed and shaken after each irradiation interval to ensure air saturation in the sample. For measurements at anoxic conditions the dye solution in the cuvette was bubbled through with argon for ten minutes prior to the experiment. The cuvette was unsealed after each irradiation interval, and the solvent was refilled to compensate its loss caused by the argon bubbling. Before starting the next irradiation/measurement cycle the dye solution was again deoxygenated by argon bubbling for 3 minutes.

Cyclic voltammetry measurements

Cyclic voltammetry measurements were performed with 1 mM dye concetration in 0.05 M tetrabutylammonium perchlorate in dry CCl_2H_2 as the supporting electrolyte at a 1.6 mm diameter Au disk electrode (BAS Inc.) at a scan rate of 0.1 $V \cdot s^{-1}$.The working electrode was polished with 0.05 µm Alumina, rinsed with dry ethanol, and dried under vacuum. Pt and Ag wires served as the counter and pseudo reference electrode, respectively. The reference potential was calibrated versus the ferrocene/ferrocenium (Fc/Fc^+) couple. The measurement cell and electrolyte were purged with argon prior to the measurements. All measurements were done inside an Ar filled glove box (MBraun) in the dark using a Biologic SP-300 electrochemical work station.

Oxygen response of the polystyrene sensors

Calibration of all sensors was carried out using a Firesting oxygen meter form PyroScience. The modulation frequency for all the Pt(II)-dyes was 4 kHz, whereas the modulation frequency for all the Pd(II)-dyes was 500 Hz. The composition of the gas was adjusted using a custom-build gas-mixing device based on mass-flow controllers from MKS (Munich, Germany) and Voegtlin (Hamburg, Germany) by mixing compressed air, nitrogen and oxygen. Temperatures were controlled and kept constant by a cryostat ThermoHaake DC50.

Upconversion experiments

Upconversion measurements were performed on FluoroLog® 3 spectrofluorometer from Horiba. Besides excitation of the sensitizer-annihilator solutions in toluene with a 450 W xenon lamp (standard), a laser diode (635 nm, from Roithner-Laser.com) was used. Due to the high concentration of the sensitizer-annihilator solutions all spectra were recorded in the front-face mode. All solutions were deoxygenated in a screw-cap cuvette (Hellma; Müllheim, Germany) by bubbling argon through the solution for 10 minutes. For the kinetic measurements the following transmission filters (50%, 25%, 10%, 5%) were used. The quantum yields of the upconverted fluorescence were roughly estimated by comparing the emission of the annihilator

and the emission of the sensitizer without the annihilator as well as the emission of an 5,5-difluoro-1,3,7,9-tetraphenyl-5H-4l4,5l4-dipyrrolo[1,2-c:2',1'-f][1,3,5,2]triazaborinine [34] used as a reference. The photographic images of the upconverted fluorescence were acquired using 635, 650 and 675 laser diodes (Roithner) with Canon 5D camera.

3. Results and Discussion

Synthesis

The platinum(II) and palladium(II) complexes of the octa- and tetra-sulfone dyes (Pt(II)-O-S, Pt(II)-T-S) were conveniently prepared in only four steps following the template method (Scheme 1). Generally, template condensation starting from very cheap and readily available chemicals such as phthalimide and phenylacetic acid represents an alternative way to Lindsey method [30]. However, this method was often reported to produce a number of side products (benzyl-substituted porphyrins), which are extremely challenging to remove. [35], [36] Moreover, not all compounds are suitable for the use in template condensation, since they must tolerate very high temperatures (340-360 °C). Recently, Müller et al. [37] reported a new method yielding analytically pure benzoporphyrins in which phthalonitrile was used instead of phthalimide with the condensation performed at only 280 °C. The new method was adapted for the synthesis of Pt(II)-O-S and Pt(II)-T-S dyes using 4,5-bis((2-ethylhexyl)thio)phthalonitrile or 4-((2-ethylhexyl)thio)phthalonitrile, respectively, as starting compounds (Scheme 1). The phthalonitriles were reacted with 4-fluorophenylacetic acid in presence of zinc phenylacetate to give the thio-substituted zinc porphyrins in 6% and 4% yield for 4,5-bis((2-ethylhexyl)thio)phthalonitrile or 4-((2-ethylhexyl)thio)phthalonitrile, respectively. Although such yields may appear low at the first glance, they allow preparing the benzoporphyrins on a multi-gram scale, considering availability of the starting compounds and extreme simplicity of the procedure. Importantly, attempts to use the 4,5-bis((2-ethylhexyl)sulfonyl)phthalonitrile as starting compound were not successful due to formation of phthalocyanine instead of the benzoporphyrin.

Metal-free thio-substituted porphyrins were obtained by demetalating the zinc complexes in acidic media (4M HCl). They were oxidized by excess of meta-chloroperoxybenzoic acid to the respective sulfone-substituted porphyrins in about 50% yield and finally converted to the metal complexes using Pt(II) and Pd(II) dichlorodibenzonitrile complexes as precursors.[35], [37] NMR and mass spectrometry (Fig. S 35-73, ESI) confirmed the identity and purity of the compounds and showed that no other products (such as benzyl-substituted side products or partly oxidized porphyrins) were formed. Note that thio-substituted zinc complexes and the

metal-free porphyrins are prone to oxidation (particularly in presence of light), requiring particular care during purification and storage.

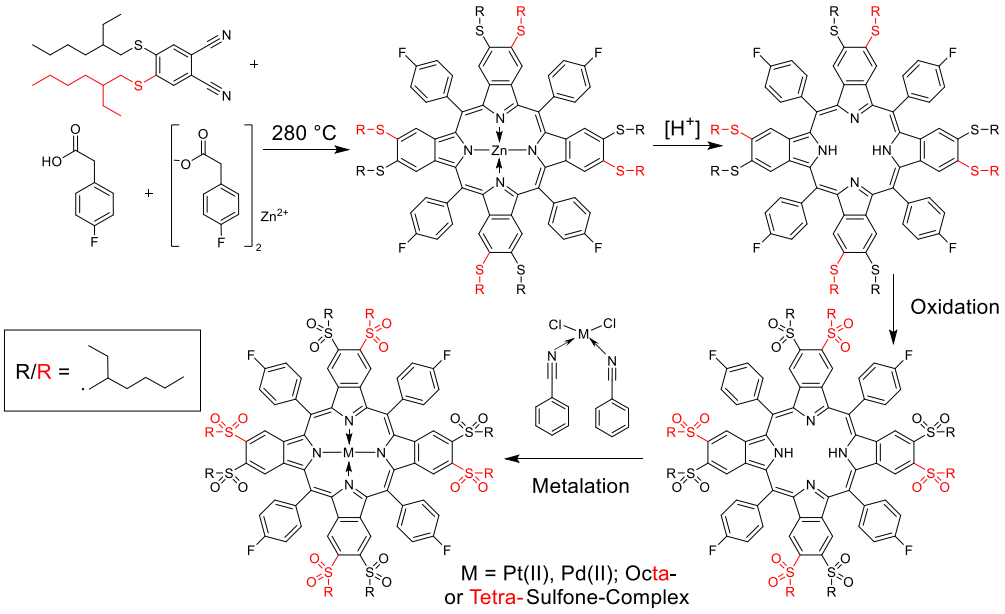

Scheme 1. Synthesis of the Pt(II) / Pd(II)-T-S and O-S benzoporphyrins.

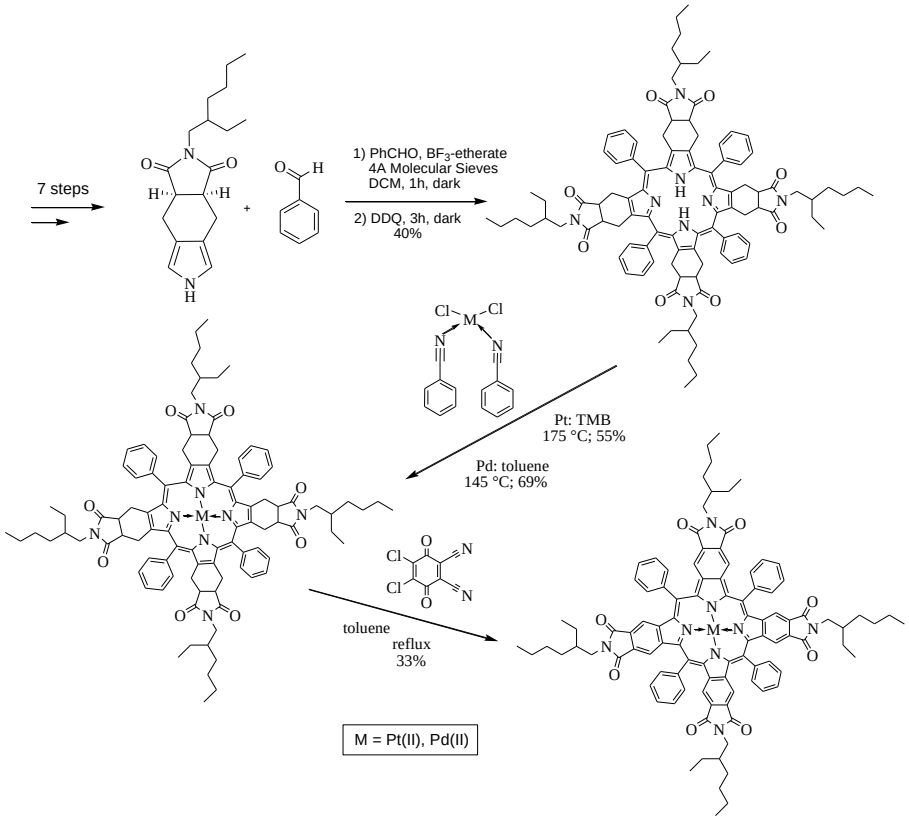

Scheme 2. Synthesis of the Pt(II)/ Pd(II)-T-I dyes.

Additionally, we prepared imide modified Pt(II) benzoporphyrin following a procedure (Scheme 2) modified to the one of Zems et al. [4] , which required 10 synthetic steps (ESI). The Pd(II) analog was also synthesized. Compared to the tetra- and octasulfone benzoporphyrins, the

synthesis of the tetra-imide dyes is significantly more challenging and time consuming due to high synthetic effort, the high costs and poor availability of necessary chemicals such as tert-butyl-isocyanoacetate.

Electrochemical properties

Table 1 provides an overview of half-wave potentials obtained for the new complexes as well as for Pt(II) and Pd(II) complexes with TPTBP used as references (the cyclic voltammograms can be found in the ESI, Fig. S1-8). The half-wave potentials $E_{½}$ increase with increasing electron-withdrawing effect of the substituents in the order TPTBP < tetra-sulfone < tetra-imide < octa-sulfone. The same trend was observed in case of fluorinated (benzo)porphyrins.[33], [38] The positive shift for all the synthesized dyes indicates a significantly lowered HOMO, resulting in improved oxidation stability due to the lowered electron density at the metalloporhyrin core. In all cases at least two reversible one-electron reductions and two reversible one-electron oxidations were observed. The obtained half-wave potentials for the Pt-T-Idyes correlate well with the data of Zems et al. [4] Pt-O-S, which oxidation potential is again 0.2 V more positive compared to Pt-T-I appears to be the most electron-deficient benzoporphyrin reported to date and have their potential increased by nearly 0.7 V compared to Pt-TPTBP.

Table 1. Half-wave potentials (V vs. Fc/Fc^{+}) of benzoporphyrin complexes in DCM containing 0.1 M $TBAClO_4$ at a scan rate of 0.1 $V \cdot s^{-1}$.

Dye	$E_{½\ red.}$ 3	$E_{½\ red.}$ 2	$E_{½\ red.}$ 1	$E_{½\ ox.}$ 1	$E_{½\ ox.}$ 2	$E_{½\ ox.}$ 3
Pt-O-S	-2.03	-1.65	***-1.17***	***0.89***	1.18	-
Pd-O-S	-2.09	-1.70	***-1.24***	***0.79***	1.01	-
Pt-T-S	-	-1.98	***-1.57***	***0.60***	1.02	-
Pd-T-S	-	-1.87	***-1.50***	***0.57***	0.89	1.26
Pt-T-I	-1.99	-1.69	***-1.39***	***0.69***	1.05	-
Pd-T-I	-2.00	-1.67	***-1.40***	***0.64***	0.89	-
Pt-TPTBP	-	-	***-1.84***	***0.21***	0.83	1.43
Pd-TPTBP	-	-2.23	***-1.84***	***0.16***	0.66	-

Photophysical Properties

As expected, all the complexes show very good solubility in organic solvents including in solvents as apolar as cyclohexane. In contrast, the dyes are poorly soluble in methanol and other polar solvents and are insoluble in water. Figure 1 shows the spectral properties of the new Pt(II) and Pd(II) benzoporphyrin complexes. The dyes efficiently absorb in the blue (Soret band) and the red (Q bands) withexceptionally high molar absorption coefficients (Table 2). The absorption bands for the Pd(II) complexes are bathochromically shifted by about 15 nm compared to their Pt(II) analogs. The absorption bands shift bathochromically in the order tetra-sulfone < octa-sulfone < tetra-imide. For comparison, the absorption bands of the non-substituted Pd(II)-TPTBP and Pt(II)-TPTBP complexes [39] are located at shorter wavelengths than those of the tetra-sulfone complexes (Table 2). Thus, the new dyes offer significant improvement over TPTBP complexes: (i) The absorption of the Pt(II) complexes becomes compatible to the emission of 455 and 465 nm LEDs, which are amongst the brightest LEDs available. Upon excitation with blue light the new dyes can be viewed as ultra-bright mega-Stokes emitters. (ii) The Q-band of the Pt-O-S complex and particularly of the T-I complex show excellent compatibility with the light of He-Ne lasers (632.8 nm) and of red laser diodes (635 nm), thus enabling a variety of potential applications (e.g., in *vivo* imaging). (iii) The Pd-T-I complex having the longest absorption wavelength is a promising alternative to naphthoporphyrin complexes.

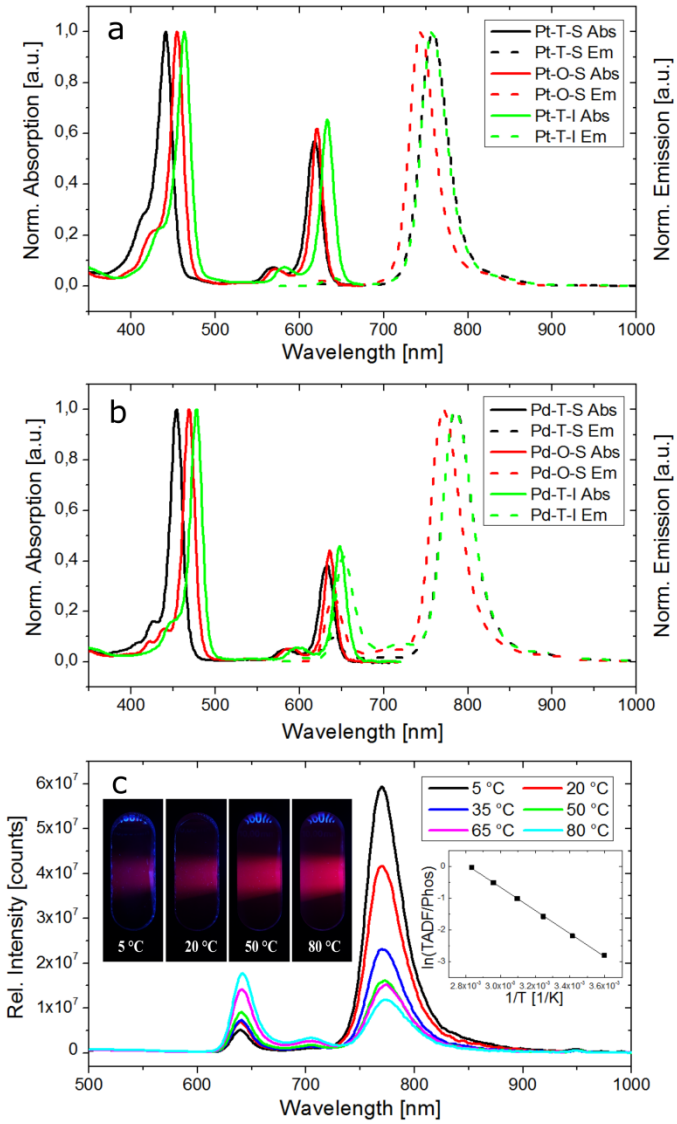

Figure 1. a,b) Absorption (solid lines) and emission (dashed lines) spectra of Pt(II) and Pd(II) complexes in toluene, respectively. T = 25 °C; anoxic conditions for emission measurements; c) Temperature dependency of the emission spectra of Pd-O-S in anoxic toluene; the inserts show the photographic images of the solution under excitation with 465 nm LED and the Arrhenius dependence for the ratio of TADF and phosphorescence.

Table 2. Photophysical properties of the Pt(II) and Pd(II) complexes in toluene solution at 25 °C**.**

Dye	Abs. λ_{max} (ε) [nm ($l \cdot mol^{-1} \cdot cm^{-1}$)]	Em. λ_{max} TADF [nm]	Em. λ_{max} phos [nm]	$\Delta E(S_1\text{-}T_1)$ [cm^{-1}][(a)]	Φ_{TADF}	Φ_{Phos}	τ_0 Phos. [µs]
Pt-TPTBP	430 (205.000); 614 (136.000)	620	770	3142	0.002	0.51[(b)]	47

Pt-T-S	441 (255.000); 619 (145.000)	624	756	2798	0.004	0.64	41
Pt-O-S	455 (370.000); 621 (229.000)	625	742	2523	0.014	0.77	33
Pt-T-I	463 (283.000); 633 (184.000)	639	755	2404	0.007	0.27	12
Pd-TPTBP	443 (416.000); 628 (173.000)	635	800	3248	0.009	0.21[(b)]	286
Pd-T-S	454 (328.000); 633 (125.000)	639	786	2927	0.023	0.33	157
Pd-O-S	469 (446.000); 636 (195.000)	640	772	2672	0.088	0.48	161
Pd-T-I	478 (390.000); 648 (179.000)	652	786	2615	0.024	0.08	53

(a) – calculated from the difference of λ_{max} for TADF and phosphorescence bands
(b) – Ref. [33]

Interestingly, the Pt-O-S dye in dimethylformamide (DMF) solution shows an unexpected semi-reversible transformation upon addition of the basic tetra-octyl ammonium (TOA) hydroxide solution (20% in MeOH). A strong bathochromic shift of the absorption spectra (91 nm for the Soret-band and 193 nm for the Q-band) is accompanied by a color change of the dye solution from green to pink (Fig. S9). This effect is most likely caused by the highly electron deficient properties of the dye, since similar behavior was also detected for the Pd-O-S and Pt-T-S dye, but not Pt-TPTBP. A similar behavior was observed in other solvents such as THF or pyridine and with other bases such as tetra-butyl ammonium (TBA) hydroxide (pK_a of OH^- = 17) and tetra-butyl ammonium fluoride (pK_a of HF = 3). This reaction is semi-reversible and adding traces of an acid (CF_3COOH or HCl) regenerates the original absorption spectra (Fig. S10). The semi-reversible nature of this reaction suggests nucleophilc substitution by the anion (OH^- or F^-) as the possible mechanism. The original aromatic NMR signals (7.75 – 8.5 ppm) including two signals in the aliphatic region (CH_2-group close to the sulfur at 3.6 ppm and the neighboring CH-group at 1.8 ppm) are lost (Fig. S29-34, ESI) upon stepwise addition of TOA-OH (Fig. S34, ESI) and regenerated upon addition of acid. Even though the bathochromically shifted species are in solution stable for several weeks, the reaction product could not isolated so far, limiting further investigations of this highly interesting reaction.

The new benzoporphyrin complexes show strong room-temperature phosphorescence in deoxygenated organic solvents such as toluene (Fig. 1). Remarkably, despite longer wavelength of absorption of the Q-bands compared to that of the TPTBP complexes, the emission maxima of the new dyes are shifted bathochromically (Table 2). The NIR phosphorescence is exceptionally bright for the T-S and O-S complexes with quantum yields Φ of 64 and 77% for the Pt(II) dyes and 33% and 48% for the Pd(II) dyes. Accurate determination of quantum yields in the NIR is challengingas evidenced in a wide literature. For

Pt-TPTBP, for instance reported quantum yields range from 35% or 51% in toluene (the short τ_0 of 30 µs in the latter case may indicate quenching by oxygen) [40],[33] to 67% in polyethylene glycol [41] and 70% in 2-Me-THF [23]. Therefore, we verified the literature values by estimating Φ relative to that of Indocyanine Green, which was proposed as NIR standard (Φ = 0.132 in ethanol).[42] The obtained values of 64% and 19% for Pt-TPTBP and Pd-TPTBP, respectively, are close to the values (51 and 21%, respectively) reported previously by our group [33]. For consistency with the previous results these reported values have been used here. The brightness of the new dyes (defined by the product of molar absorption coefficient and luminescence quantum yield) is very high, particularly for the O-S complexes.

The most striking feature of the new dyes, however, is thermally activated delayed fluorescence, which is particularly strong for the Pd complexes (Fig. 1b) and can already at room temperature clearly be observed by naked eye (Fig. 1c, insert). Such strong TADF is unprecedented for porphyrin complexes. For comparison, the quantum yield of TADF of Sn(IV) porphyrins was reported to be 0.6% at 23 °C and 2% at 117 °C. Note that despite a large number of recently reported dyes show efficient TADF in view of their potential applications in OLED technology, [43]–[50] those emitting in the red and NIR remain extremely rare. [51]–[54] The observed emission can be unambiguously assigned to TADF on the basis of the temperature dependence, identical decay times of TADF and phosphorescence, and the linear relation between TADF intensity and excitation intensity with a slope of 1 (ESI, Fig. S9), proofing that no other radiative process like, e.g., triplet-triplet annihilation based upconversion is involved. Interestingly, we could also record weak yet measurable TADF for Pt(II)- and Pd(II)-TPTBP complexes, which has been overseen in the previous studies involving these compounds.(Ref required?) The Pt(II) complexes show significantly less efficient delayed fluorescence than the Pd(II) analogs, which correlates well with the much shorter luminescence lifetime of the former and faster deactivation of the T_1 state via phosphorescence.

Highly efficient TADF of the new metalloporphyrins can be explained by their fairly small singlet-triplet energy gap $\Delta E_{S1\text{-}T1}$, which enables reverse inter-system crossing. $\Delta E_{S1\text{-}T1}$ decreases in the order TPTBP > T-S > O-S > T-I, which correlates well with the TADF-to-phosphorescence ratio (Table 2). This ratio is the highest for the T-I complexes (i.e., those with the lowest energy gap) despite their emission quantum yields being much lower than those of the O-S complexes. In absolute terms, the Pd-O-S complex shows the highest TADF quantum yield as is clearly visible with a naked eye even at 5 °C.

Fig. 1c (insert) shows Arrhenius dependence for the TADF-to-phosphorescence ratio. It allows estimating the activation energy ΔE according to the equation of Parker and Hatchard [55]:

$$\frac{\Phi_{TADF}}{\Phi_{Phos}} = \tau_0 \cdot \Phi_F \cdot A \cdot e^{-\frac{\Delta E}{kT}} \quad (1)$$

where τ_0 is the natural radiative lifetime of the triplet state, *A* is a frequency factor and k is the Boltzmann constant. Since the quantum yield of the prompt fluorescence was to small to be measured, only ΔE was calculated. The plots of $\ln(\Phi_{TADF}/\Phi_{Phos})$ against 1/T are linear as predicted (correlation coefficient 0.9994). ΔE was obtained to be 30.1 kJ·mol^{-1} or 2520 cm^{-1}, which is very close to the values of the triplet-singlet energy gap obtained from the emission spectra (ΔE_{S1-T1} = 2672, Table 2).

Interestingly, the T-I complexes have with 27% and 8% for the Pt(II) and Pd(II) complex, respectively (Table 2)significantly lower luminescence quantum yield in solutions. Zems et al. [4] reported 45% for the Pt(II) tetra-imide complex, which appears to be overestimated. The non-radiative constants ($k_{nr} = (1-\Phi)/\tau$) for the T-I complexes are thus much higher than for the TPTBP, T-S and O-S complexes (Table S1, ESI).The phosphorescence decay times of the new Pt(II) and Pd(II) complexes are shorter than those of Pt-TPTBP and Pd-TPTBP, respectively, (Table 2) which together with the quantum yields indicates higher values of the radiative constant ($k_r = \Phi/\tau$). (Table S1, ESI).

Photostability

This property is of particular interest for practical applications, where high light intensities are applied for long time such as in upconversion. The benzoporphyrin derivatives may become unstable against oxidation and reduction by the destabilization of the third LUMO and the first HOMO of the porphyrin due to π-ring expansion.[56] Photostability of naphthoporphyrins and their molecular hybrids with benzoporphyrins is particularly low.[32]

Preliminary experiments revealed very poor photostability of the thio-substituted Zn-complex (Zn-O-T) in air-saturated solution, which might be due to oxidation of the macrocycle by photosensitized singlet oxygen promoted by the electron-donating character of the thio-groups. Indeed, the zinc complex was almost completely destroyed within 7 minutes irradiation with a blue LED array (λ_{max}=458 nm; 10.79 V, 0.689 A, 7.4 W) (Fig. S10, ESI). Interestingly, photostability of the complex in anoxic toluene is similarly poor (Fig. S11, ESI), suggesting that intramolecular redox processes are the main degradation route of the excited dye. High photostability of the T-S and O-S benzoporpyhrins was expected due to the strong electron-withdrawing effect of these substituents. Similarly, excellent photostability was shown for the Pt(II)-tetra-imide complex.[4] Photostabilty of the complexes was investigated by monitoring

their absorption upon continuous irradiation for six hours in air-saturated toluene at 25 °C with a high power 617 nm LED (Figure 4).

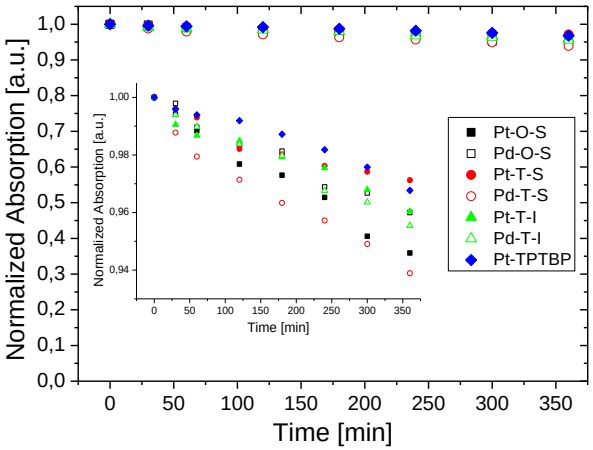

Figure 3. Photodegradation profiles for the metalloporphyrins in air-saturated toluene solution at 25 °C upon irradiation with a high power 617 nm LED (28 V, 550 mA, photon flux: 18.000 µmol s^{-1} m^{-2}; irradiance 350 mW·cm^{-2}).

Pt-TPTBP, which is widely used in sensing and upconversion applications, was used as reference. All the dyes are highly photostable and only marginal changes (within the measurement inaccuracy) are observed upon prolonged illumination with high light intensity. The results indicate that the photostability is similar for all new dyes (Fig. 3). The photobleaching rates were also similar to the photodegradation rate of Pt-TPTBP, which does not agree with the results reported by Zems et al. (about 5 times faster bleaching of Pt-TPTBP compared to Pt-T-I) who, however, used much harsher conditions (irradiation with 500 W halogen lamp at 90 °C). Furthermore, Pt-T-S and Pt-O-S show equally hardly any change in the absorption over 6 hours irradiation in anoxic toluene (Fig. S11, ESI).

The nature of the solvent plays a crucial role with for the photobleaching rates. For example, Pt-O-S and Pt-TPTBP were almost completely destroyed after 15 min irradiation in dimethylformamide (Fig. S12, ESI), where photoreduction may be a predominant photodegradation mechanism. Therefore, the choice of suitable solvents or matrices is extremely important to achieve the best performance in the respective application.

TADF of the polymer-immobilized dyes

Immobilizing the dyes in polymers is essential for the design of optical oxygen sensors. Although the new dyes can be embedded in a variety of polymers, polystyrene was chosen as a model substrate due to its good optical properties, adequate chemical stability and moderate oxygen permeability, which makes it widely used in the sensor community. Moreover, many

nanoparticle-based materials are available on basis of polystyrene and its co-polymers, which is very useful for designing optical nanoprobes. Fig. 4 confirms similar photophysical properties of the polystyrene-immobilized and dissolved dyes. Although NIR phosphorescence dominates the emission at room temperature, TADF is clearly visible for the Pd(II) complexes (Fig. 4b). With Pd-O-S and Pd-T-I the phosphorescence is almost entirely converted to TADF at temperatures 120 °C (Fig. 4c, video ESI). Interestingly, even Pd-TPTBP shows fairly strong TADF under these conditions, confirming that the observed phenomenon is general for all presented porphyrin complexes. In full agreement with the values of the singlet-triplet energy gap and the solution measurements, the TADF-to-phosphorescence ratio is the highest for Pd-T-I, followed by Pd-O-S, Pd-T-S and finally Pd-TPTBP (Table 3). This ratio increases for all complexes about 10-fold from 23-26 °C to 116-130 °C (Table 3). Again, Pd-O-S becomes the "champion" due its higher quantum yields.

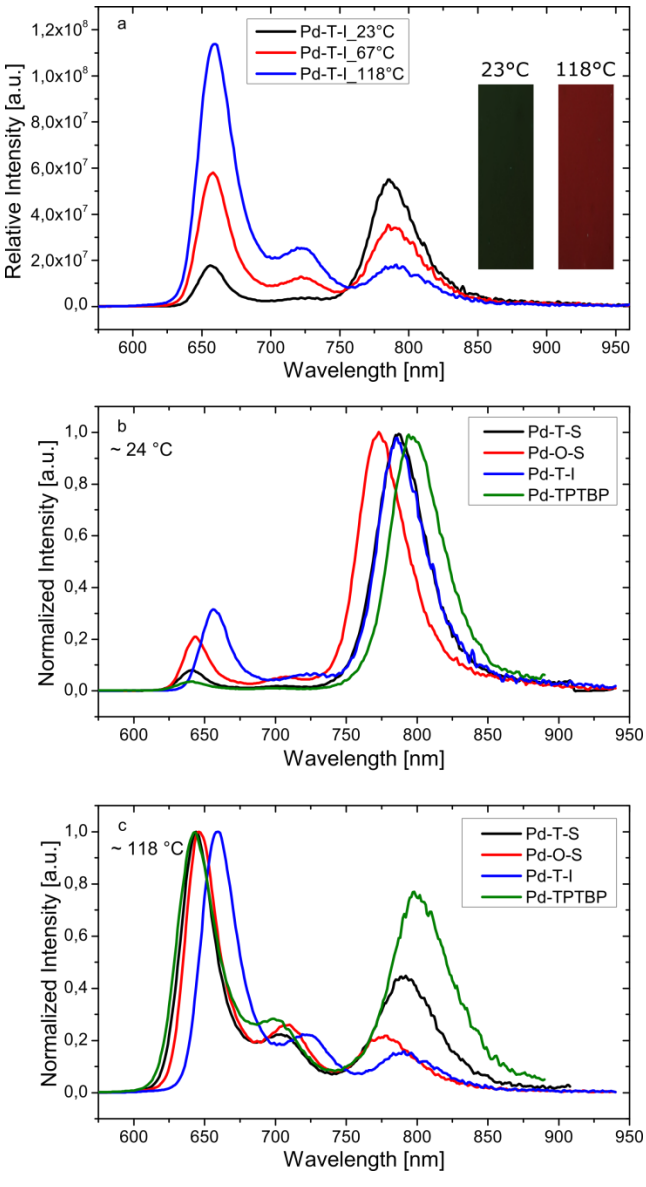

Figure 4. (a) Temperature dependency of the emission spectra of Pd-T-I in polystyrene and photographic images of the same material at 23 and 118 °C excited with an UV-Lamp at 365 nm (all under N_2 atmosphere); (b) Normalized emission spectra of Pd-T-S, Pd-O-S, Pd-T-I and Pd-TPTBP at 23 - 25 °C and (c) at 116 - 130 °C in polystyrene under N_2 atmosphere.

Table 3. Quantum yields of thermally activated delayed fluorescence (TADF) and phosphorescence of selected dyes in polystyrene matrix.

dye	Temp. [°C]	Φ_{TADF}	Φ_{Phos}	$\Phi_{TADF/Phos}$
Pd-T-S	23	0.006	0.088	0.068
	116	0.062	0.039	1.590
Pd-O-S	23	0.019	0.121	0.157
	120	0.169	0.052	3.250
Pd-T-I	23	0.020	0.077	0.260
	118	0.143	0.031	4.613
Pd-TPTBP	26	0.003	0.072	0.042
	120	0.038	0.036	1.056
Pt-O-S	26	0.009	0.393	0.023
	130	0.077	0.213	0.362
Pt-TPTBP	27	0.001	0.255	0.004
	133	0.016	0.116	0.138

Optical Oxygen Sensors

Optical oxygen sensing is undoubtedly one of the most important applications of porphyrin complexes. Since phosphorescence is a predominant process at ambient temperature, only phosphorescence quenching was investigated. Fig. 5 shows the Stern-Volmer plots for polystyrene-immobilized dyes. The non-linear plots can be described by a "two-site model" [57], which assumes localization of an oxygen-sensitive chromophore in two microenvironments (resulting from micro-inhomogeneities in the polymer) possessing different gas permeabilities:

$$\frac{I}{I_0} = \frac{\tau}{\tau_0} = \frac{f}{1+K_{SV1}*[O_2]} + \frac{1-f}{1+(K_{SV1}*m)*[O_2]} \qquad (2)$$

f is the fraction of the total emission of the first environment; K_{SV1} and K_{SV2}=(K_{SV1}·*m*) are the Stern-Volmer constants for the two environments. The obtained fit parameters are summarized in Table 4. As expected from the τ_0 values, the sensitivity of the Pd(II) complexes is significantly higher than that of the Pt(II) complexes. While the polystyrene optodes based on the Pt dyes are best suitable for measurements from 1 to 1000 hPa O_2, the Pd(II) based sensors make much lower oxygen partial pressures accessible. The sensing behavior of the octa- and tetra-sulfone complexes is very similar (Fig. 4, Table 4). The Stern-Volmer plots for the tetra-imide

dyes are significantly more linear, which indicates higher homogeneity of the environment. The sensitivity can be further greatly increased by immobilizing the complexes into matrixes with higher oxygen permeability. For example, immobilizing into highly permeable silicone rubbers to design trace sensors is enabled by the excellent solubility of the dyes, which avoids the need for their chemical modification to prevent aggregation via covalent entrapment. [58]

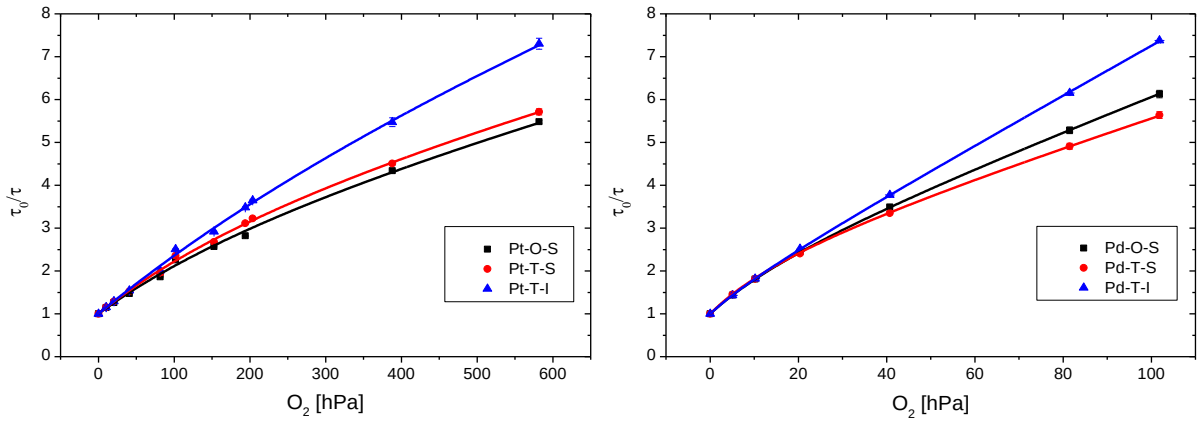

Figure 5. Stern-Volmer plots of the phosphorescence for the Pt(II) and Pd(II) complexes embedded in polystyrene (at 25 °C).

Despite our expectations that the highly soluble dyes can be uniformly dispersed into polymers in a high concentration, we found strongly decreased phosphorescence decay times with highly loaded polymers (Fig. S10, ESI); increasing the Pt(II) complex concentration from 2 to 5 wt.% decreased the lifetime by 7% for Pt-O-S, 10% for Pt-T-S and 15% for Pt-T-I. Less soluble Pt-TPTBP showed much smaller τ_0 decrease at 2% loading despite its higher molar concentration. The same trend was observed at 20wt.%, where the lifetime decreased by 41% for Pt-O-S and Pt-T-S, 53% for Pt-T-I, but only 17% for Pt-TPTBP. It is likely that smaller molecules such as Pt-TPTBP, dissolve more easily and aggregate less in polystyrene, whereas more sterically demanding dyes tend to aggregate by formating apolar microdroplets, which separate from the polymer phase. The results likely differ in apolar matrixes such as silicones, which show better compatibility with the new dyes than the TPTBP complexes. Still, the concentration range where aggregation in polystyrene is negligible isfully adequate for manufacturing of oxygen sensors.

Table 4. Photophysical and oxygen sensing properties of Pt(II) and Pd(II) benzoporpyhrin complexes in polystyrene.

Dye		**f**	**m**	**K_{SV} [hPa^{-1}]**	**τ_0 [µs]**	

	absolute Φ [%][(a)]			10 °C	25 °C	40 °C	10 °C	25 °C	40 °C	temp. coeff. at 25 °C [%τ_0/K]
Pt-O-S	39.3	0.860	0.054	0.012	0.015	0.019	46.5	45.9	45.1	0.102
Pd-O-S	12.1	0.767	0.101	0.099	0.119	0.142	350	328	308	0.421
Pt-T-S	27.5	0.868	0.043	0.014	0.017	0.020	50.1	49.5	48.7	0.097
Pd-T-S	8.8	0.738	0.075	0.115	0.130	0.144	379	360	338	0.376
Pt-T-I	23.3	0.945	0.031	0.013	0.015	0.018	41.9	40.8	39.5	0.204
Pd-T-I	7.7	0.659	0.213	0.115	0.130	0.144	287	265	244	0.537

(a) Phosphorescence quantum yields.

Accelerated photostability tests of the polystyrene sensors were performed by positioning sensor spots (5 mm diameter) onto a distal end of a plastic fiber connected to the read-out device from PyroScience (624 nm LED, 100% LED intensity, 100 ms integration time). Under anoxic conditions, the luminescence intensity decreased at most 0.502% per 2500 measurement points for Pt-O-S and 0.349% per 2500 measurement points for Pd-O-S. With air saturation Pt-O-S decreased in average by 1.31% per 2500 measurement points in the first 500 minutes and slowed down thereafter to 0.18% per 2500 measurement points from 500 to 1000 minutes. Note that integration over 10 ms and 10% LED intensity (1% of the light dose used in accelerated tests) are sufficient to acquire a measurement point, which indicates suitability of the sensors for very long measurements. Further improvement may be possible by optimizing the polymer matrix, since the decrease in luminescence intensity and decay time are more likely caused by quenching groups formed in the proximity of the dye (caused by reaction of the photosensitized singlet oxygen with the polymer) rather than by dye bleaching itself.

Application As Dual Oxygen And Temperature Sensor

As mentioned above, simultaneous oxygen and temperature sensing is of high importance for practical applications and essential for precise oxygen quantification. So far, the oxygen probe to be combined with a temperature probe that was either fully independent or combined in a dual-sensing material. o by. The unique dual phosphorescence and TADF of the new dyes makes them suitable for simultaneously sensing oxygen and temperature with a single probe, which we. demonstrate with the Pd-O-S complex since it has the strongest TADF. Since polystyrene is too oxygen permeable to measure the most relevant concentration range between 0 and 210 hPa it was substituted by a commercially available styrene-acrylonitrile copolymer (PSAN, 25 wt% acrylonitrile) featuring lower oxygen permeability ($P = 3.5 \cdot 10^{-14}$ $cm^2 \cdot Pa \cdot s^{-1}$ compared to $1.9 \cdot 10^{-13}$ $cm^2 \cdot Pa \cdot s^{-1}$ for polystyrene).

Fig. 6 shows that simultaneous oxygen and temperature sensing is indeed possible with this arrangement. NIR phosphorescence is gradually replaced by TADF as the temperature increases (Fig. 6a and 6b). This effect is very similar for both extremes: anoxic conditions (Fig. 6a) and air-saturated conditions (Fig. 6b). Interestingly, in the second case the intensity of TADF at 125.4 °C is lower than that at 113.4 °C, which might be due to increased oxygen quenching efficiency above the T_g of the polymer at 104-127 °C [59], [60]. Figure 6c shows that the TADF-to-phosphorescence ratio is virtually independent of pO_2 and thus serves as a self-referenced analytical parameter for temperature measurement. The decay time profiles (Fig. 6d) are mono-exponential in the absence of oxygen but become bi-exponential in its presence, which is not uncommon for optical oxygen sensors. Therefore, average lifetimes were calculated via $\tau_{av} = \frac{\sum_{i=1}^{n} B_i T_i^2}{\sum_{i=1}^{n} B_i T_i}$ where the B_i is the pre-exponential factor and T_i the individual lifetimes. Importantly, the decay time traces are identical for phosphorescence and TADF. This allows determining the second parameter (pO_2) in the lifetime mode. Depending on the temperature and therefore on the intensity of the respective luminescence component either phosphorescence (lower temperatures) or TADF (higher temperatures) can be analyzed to maintain the best S/N ratio. The decay times decrease with temperature at all oxygen concentrations (Fig. 6e). The Stern-Volmer plots (Fig. 6f) are typical for oxygen sensors with higher quenching efficiency at elevated temperatures despite comparably strong shortening of τ_0 in these conditions. As expected, the oxygen sensitivity is lower than in polystyrene (Fig. 5). In summary, combination of the decay time and ratiometric read-out allows to access information about both oxygen and temperature with a single indicator dye. Importantly, both measurements are self-referenced. Further improvements can include increasing the acrylonitrile fraction in the PSAN copolymer which would reduce the quenching by oxygen to a more optimal value (τ_0/τ ~3-4 at air saturation). Further modifying the indicator for an even higher TADF fraction already at RT would be desirable to enable reliable dual sensing below 20 °C. With the current system TADF below 20 °C and air saturation might be too weak to be reliably quantified with compact devices based on photodiodes although, as demonstrated above, this represents no problem for the photomultiplier-based set-up.

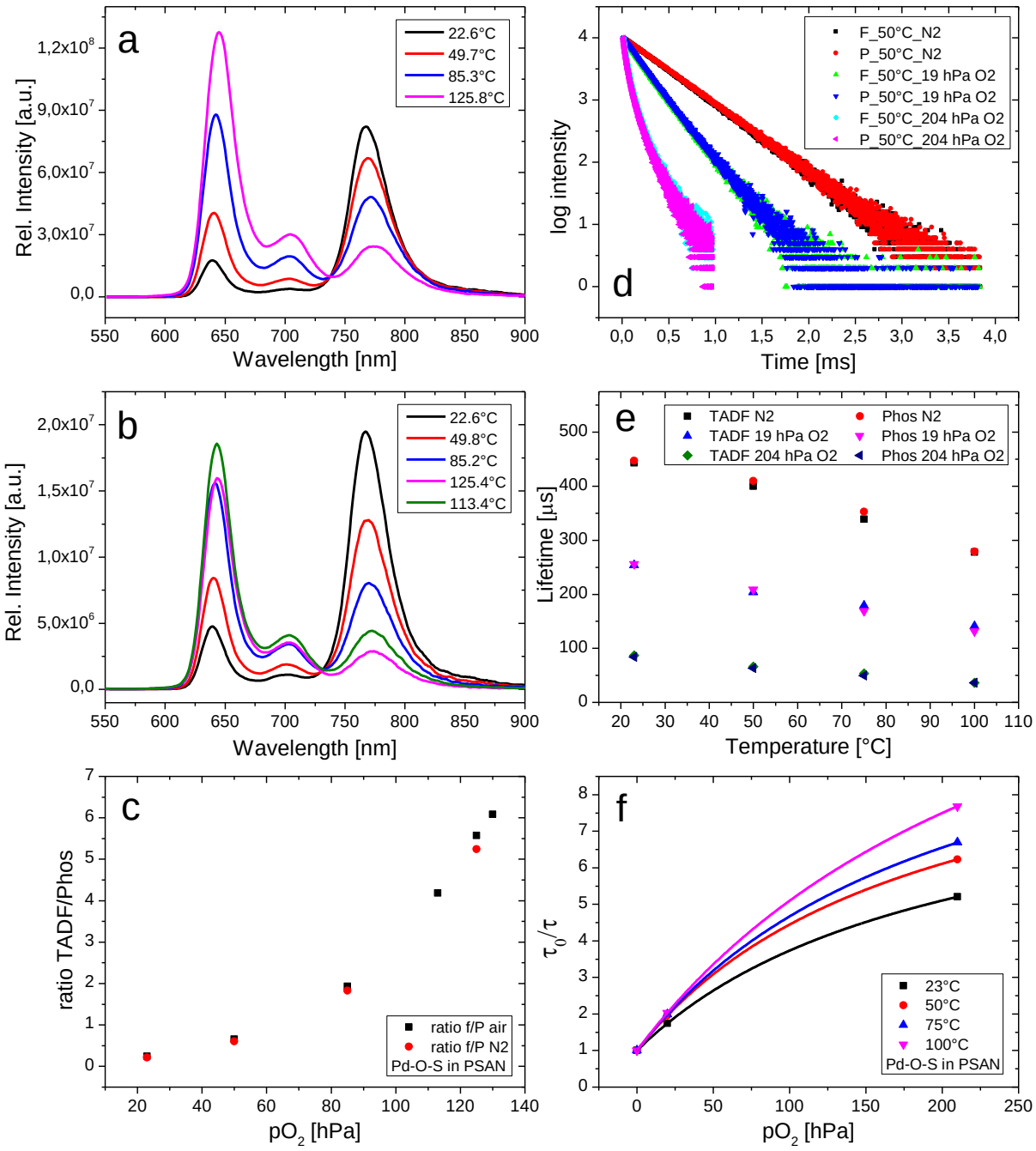

Figure 6. (a) and (b): temperature dependency of the emission spectra of Pd-O-S in PSAN under anoxic conditions air saturation, respectively. Note that slits of fluorometer were different for both conditions; c: calculated ratio of TADF and phosphorescence at different temperatures for the same conditions; d: examples of the decay curves of TADF and phosphorescence at 50 °C; e: temperature and oxygen dependency of the lifetimes of TADF and phosphorescence; f: Stern-Volmer plots at different temperatures.

Dyes as Sensitizers in Triplet-Triplet-Annihilation-Based Upconversion Systems

Triplet-triplet annihilation-based upconversion (TTA) has recently attracted much attention in the scientific community since it may enable exploiting low-energy long wavelength radiation in photovoltaics. TTA relies on a sensitizer (S), which should efficiently absorb light at a given wavelength and transfer its energy to an annihilator (A), generating higher energy fluorescence *via* triplet-triplet annihilation [17]. The sensitizer is required to have a high molar absorption coefficient, high efficiency of intersystem crossing [17], and the long lifetime necessary for efficient triplet-triplet energy transfer. Particularly, excitation in the red to NIR is highly interesting because of the considerable solar power and low photovoltaics efficiency in this region.[19]–[22] Additionally, good solubility in organic solvents and polymers and high photostability are essential. The new benzoporphyrin derivatives fulfil these requirements are almost perfectly. Their sensitizing capabilities were investigated in anoxic toluene solutions containing $1{\cdot}10^{-4}$ M sensitizer (perylene dyes, structures Fig. S ESI) and $5{\cdot}10^{-4}$ M annihilator. Figure 7, Table S2, and Fig. S1-12 (ESI) show that all new dyes perform as efficient sensitizers for the upconverted fluorescence. Quadratic dependence of fluorescence on excitation intensity (xenon lamp) was be observed for all dyes (Fig. S14-25, ESI) using the (slope approximately 2) as is typical for nonlinear processes like TTA based upconversion.[18], [21], [61]–[63] Measurements conducted with the 635 nm laser diode reveal a linear region with a slope of unity indicating saturation conditions. [64]

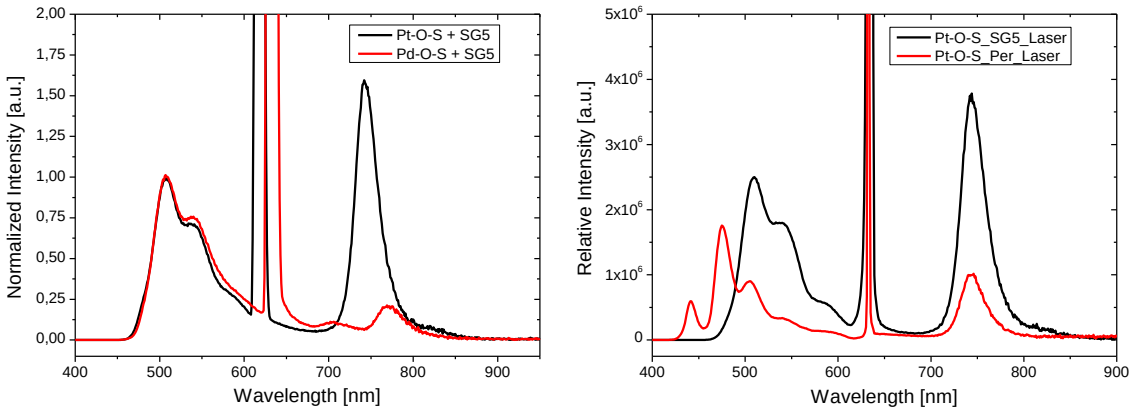

Figure 7. Emission spectra of $1{\cdot}10^{-4}$ M Pt/Pd-O-S in toluene in presence of $5{\cdot}10^{-4}$ M Solvent Green 5 (SG5) as annihilator when excited with a 450 W xenon-lamp (a) and $5{\cdot}10^{-5}$ M Pt-O-S in toluene containing either $2.5{\cdot}10^{-4}$ M SG5 or perylene when excited with a 635 nm laser diode.

The sensitizing efficiency of the new dyes is similar or better (for the O-S complexes) to that of the TPTBP derivatives used in many studies so far.

A notable advantage of the T-I and O-S dyes is that they enable sensitizing the upconverted fluorescence at significantly longer wavelengths than the TPTBPs (Fig. 8). As suggested by

the absorption spectra, Pd-T-I can efficiently sensitize upconverted fluorescence even at 675 nm excitation. For comparison, a Pd(II) complex with mono-naphtho-tribenzo-tetraphenyl-porphyrin [29], found to be very useful in upconversion applications, [65] absorbs at similar wavelenghts, albeit with significantly lower molar absorption coefficients,bathochromically shifted emission (λ_{max} = 849 nm), and the limitation of moderate photostability.[29] A small singlet-triplet energy gap also enables sensitizing for annihilators with at rather long emission wavelengths such as Lumogen orange (Fig. 8).

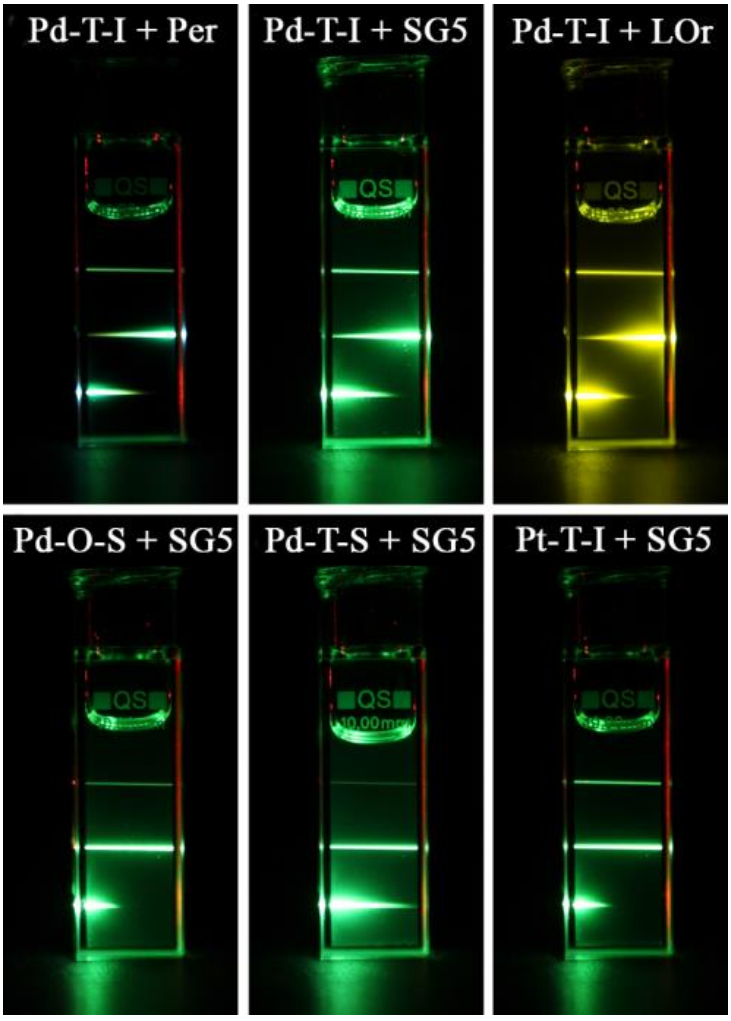

Figure 8. Photographic images of $5 \cdot 10^{-5}$ M deoxygenated toluene solutions of various sensitizers and different annihilators (C = $2.5 \cdot 10^{-4}$ M; Per=perylene, SG5=solvent green 5 & LOr=Lumogen orange) upon excitation with several laser diodes (675 nm, 650 nm and 635 nm, top to bottom).

Conclusions

Highly electron-deficient platinum(II) and palladium(II) benzoporphyrin complexes bearing alkylsulfone groups have been conveniently prepared in a four step synthetic route (template method), starting from cheap and readily available materials. This contrast to a 10 step synthesis of structurally related electron-deficient tetra-imide complexes via the Lindsey pathway from expensive educts. The new platinum(II) and palladium(II) complexes can be efficiently excited in blue and in red and are compatible with many popular excitation sources (ultrabright blue and red LEDs, He-Ne laser and red laser diodes). Additionally, the new porphyrins are highly organo soluble in various solvents including cyclohexane and polystyrene and show very good photostability. The dyes show thermally activated delayed fluorescence (TADF) and strong phosphorescence in the NIR region at room temperature, which qualifies them for optical oxygen sensors. Particularly the Pd(II) complexes have already at room temperature fairly efficient TADF, which dramatically increases with temperature to reach as much as 17% for the Pd-O-S complex at 120 °C. TADF of the new dyes is much stronger than that of state-of-the-art porphyrin complexes, which is explained by the unusually small singlet-triplet energy gap of the former.

The temperature dependence of the emission has ratiometric character and enables thus dual oxygen and temperature sensing based on a single emitter, which we for the first time demonstrate. In the dual sensor the temperature is obtained from the TADF-to-phosphorescence ratio while oxygen concentration is determined from the phosphorescence or TADF decay times, which are identical.

Finally, the platinum(II) and palladium(II) complexes were both found to efficiently sensitize triplet-triplet annihilation based upconversion. Bathochromically shifted absorption of particularly the tetra-imide dyes enables longer sensitization wavelengths compared to state-of-the-art benzoporphyrin sensitizers. Additionally, the most electron-deficient compound semi-reversibly forms NIR absorbing species in basic media, which calls for a more detailed investigation (ESI). Overall, it can be concluded that outstanding photophysical properties of the new porphyrins make them particularly interesting for a broad variety of photonic applications ranging from OLED technology via photovoltaics to two photon imaging of oxygenation of biological samples. Particularly for the last application, TADF will be of special benefit since the spectral overlap between the required NIR excitation and the emission can be avoided. in contrast to state-of-the-art phosphorescent probes, which emit in the NIRand overlap with excitation..

Acknowledgements

The support from Karin Bartl (ICTM, TU Graz) for measurements of the MS-Spectra, Prof. Hansjörg Weber (OC, TU Graz) for the NMR-Spectra; Maximilian Maierhofer, Andreas Steinegger, Matthias Schwar and Johanna Schichler for synthesis and characterization of some precursors and DI Christoph Staudinger for film editing is gratefully acknowledged. The work was financially supported by the ERC Project "Oxygen" (Grant Number 267233) and the ERC Project "SenseOcean" (Grant Number 614141). S.A.F. is indebted to the European Research Council (ERC) under the European Union's Horizon 2020 research and innovation programme (Grant Number 636069).

References

[1] T. Tanaka and A. Osuka, "Conjugated porphyrin arrays: synthesis, properties and applications for functional materials," *Chem. Soc. Rev.*, Jan. 2014.
[2] C. McDonagh, C. S. Burke, and B. D. MacCraith, "Optical Chemical Sensors," *Chem. Rev.*, vol. 108, no. 2, pp. 400–422, Feb. 2008.
[3] S. M. Borisov, G. Nuss, and I. Klimant, "Red Light-Excitable Oxygen Sensing Materials Based on Platinum(II) and Palladium(II) Benzoporphyrins," *Anal. Chem.*, vol. 80, no. 24, pp. 9435–9442, Dezember 2008.
[4] Y. Zems, A. G. Moiseev, and D. F. Perepichka, "Convenient Synthesis of a Highly Soluble and Stable Phosphorescent Platinum Porphyrin Dye," *Org. Lett.*, vol. 15, no. 20, pp. 5330–5333, Oktober 2013.
[5] M. Quaranta, S. M. Borisov, and I. Klimant, "Indicators for optical oxygen sensors," *Bioanal. Rev.*, vol. 4, no. 2–4, pp. 115–157, Nov. 2012.
[6] X. Wang and O. S. Wolfbeis, "Optical methods for sensing and imaging oxygen: materials, spectroscopies and applications," *Chem. Soc. Rev.*, vol. 43, no. 10, pp. 3666–3761, Apr. 2014.
[7] C. Staudinger and S. M. Borisov, "Long-wavelength analyte-sensitive luminescent probes and optical (bio)sensors," *Methods Appl. Fluoresc.*, vol. 3, no. 4, p. 042005, 2015.
[8] X. Wang, O. S. Wolfbeis, and R. J. Meier, "Luminescent probes and sensors for temperature," *Chem. Soc. Rev.*, vol. 42, no. 19, pp. 7834–7869, Sep. 2013.
[9] T.-W. Sung and Y.-L. Lo, "Dual sensing of temperature and oxygen using PtTFPP-doped CdSe/SiO2 core–shell nanoparticles," *Sens. Actuators B Chem.*, vol. 173, pp. 406–413, Oct. 2012.
[10] X. Zhou, F. Su, Y. Tian, R. H. Johnson, and D. R. Meldrum, "Platinum (II) porphyrin-containing thermoresponsive poly(N-isopropylacrylamide) copolymer as fluorescence dual oxygen and temperature sensor," *Sens. Actuators B Chem.*, vol. 159, no. 1, pp. 135–141, Nov. 2011.
[11] C. S. Chu and Y. L. Lo, "A Plastic Optical Fiber Sensor for the Dual Sensing of Temperature and Oxygen," *IEEE Photonics Technol. Lett.*, vol. 20, no. 1, pp. 63–65, Jan. 2008.
[12] C.-S. Chu and T.-H. Lin, "A new portable optical sensor for dual sensing of temperature and oxygen," *Sens. Actuators B Chem.*, vol. 202, pp. 508–515, Oct. 2014.
[13] C.-S. Chu and T.-H. Lin, "Ratiometric optical sensor for dual sensing of temperature and oxygen," *Sens. Actuators B Chem.*, vol. 210, pp. 302–309, Apr. 2015.

[14] L. H. Fischer, S. M. Borisov, M. Schaeferling, I. Klimant, and O. S. Wolfbeis, “Dual sensing of pO2 and temperature using a water-based and sprayable fluorescent paint,” *Analyst*, vol. 135, no. 6, pp. 1224–1229, May 2010.
[15] A. Monguzzi, J. Mezyk, F. Scotognella, R. Tubino, and F. Meinardi, “Upconversion-induced fluorescence in multicomponent systems: Steady-state excitation power threshold,” *Phys. Rev. B*, vol. 78, no. 19, p. 195112, Nov. 2008.
[16] T. N. Singh-Rachford and F. N. Castellano, “Triplet Sensitized Red-to-Blue Photon Upconversion,” *J. Phys. Chem. Lett.*, vol. 1, no. 1, pp. 195–200, Jan. 2010.
[17] J. Zhao, S. Ji, and H. Guo, “Triplet–triplet annihilation based upconversion: from triplet sensitizers and triplet acceptors to upconversion quantum yields,” *RSC Adv.*, vol. 1, no. 6, pp. 937–950, Oct. 2011.
[18] S. M. Borisov, R. Saf, R. Fischer, and I. Klimant, “Synthesis and properties of new phosphorescent red light-excitable platinum(II) and palladium(II) complexes with Schiff bases for oxygen sensing and triplet-triplet annihilation-based upconversion,” *Inorg. Chem.*, vol. 52, no. 3, pp. 1206–1216, Feb. 2013.
[19] J.-H. Kim, F. Deng, F. N. Castellano, and J.-H. Kim, “High Efficiency Low-Power Upconverting Soft Materials,” *Chem Mater*, 2012.
[20] K. Xu, J. Zhao, X. Cui, and J. Ma, “Photoswitching of triplet–triplet annihilation upconversion showing large emission shifts using a photochromic fluorescent dithienylethene-Bodipy triad as a triplet acceptor/emitter,” *Chem Commun*, Dezember 2014.
[21] T. N. Singh-Rachford, A. Haefele, R. Ziessel, and F. N. Castellano, “Boron dipyrromethene chromophores: next generation triplet acceptors/annihilators for low power upconversion schemes,” *J. Am. Chem. Soc.*, vol. 130, no. 48, pp. 16164–16165, Dec. 2008.
[22] A. Monguzzi *et al.*, “Efficient Broadband Triplet–Triplet Annihilation-Assisted Photon Upconversion at Subsolar Irradiance in Fully Organic Systems,” *Adv. Funct. Mater.*, vol. 25, no. 35, pp. 5617–5624, Sep. 2015.
[23] C. Borek *et al.*, “Highly Efficient, Near-Infrared Electrophosphorescence from a Pt–Metalloporphyrin Complex,” *Angew. Chem. Int. Ed.*, vol. 46, no. 7, pp. 1109–1112, Feb. 2007.
[24] V. V. Rozhkov, M. Khajehpour, and S. A. Vinogradov, “Luminescent Zn and Pd tetranaphthaloporphyrins,” *Inorg. Chem.*, vol. 42, no. 14, pp. 4253–4255, Jul. 2003.
[25] O. S. Finikova, A. V. Cheprakov, and S. A. Vinogradov, “Synthesis and Luminescence of Soluble meso-Unsubstituted Tetrabenzo- and Tetranaphtho[2,3]porphyrins,” *J. Org. Chem.*, vol. 70, no. 23, pp. 9562–9572, Nov. 2005.
[26] C. M. B. Carvalho, T. J. Brocksom, and K. T. de Oliveira, “Tetrabenzoporphyrins: synthetic developments and applications,” *Chem. Soc. Rev.*, vol. 42, no. 8, pp. 3302–3317, Mar. 2013.
[27] T. Ishizuka, Y. Saegusa, Y. Shiota, K. Ohtake, K. Yoshizawa, and T. Kojima, “Multiply-fused porphyrins—effects of extended π-conjugation on the optical and electrochemical properties,” *Chem. Commun.*, vol. 49, no. 53, pp. 5939–5941, Jun. 2013.
[28] B. Nacht *et al.*, “Integrated catheter system for continuous glucose measurement and simultaneous insulin infusion,” *Biosens. Bioelectron.*, vol. 64, pp. 102–110, Feb. 2015.
[29] F. Niedermair *et al.*, “Tunable Phosphorescent NIR Oxygen Indicators Based on Mixed Benzo- and Naphthoporphyrin Complexes,” *Inorg. Chem.*, vol. 49, no. 20, pp. 9333–9342, Oct. 2010.
[30] J. S. Lindsey, H. C. Hsu, and I. C. Schreiman, “Synthesis of tetraphenylporphyrins under very mild conditions,” *Tetrahedron Lett.*, vol. 27, no. 41, pp. 4969–4970, 1986.

[31] M. G. Walter, A. B. Rudine, and C. C. Wamser, “Porphyrins and phthalocyanines in solar photovoltaic cells,” *J. Porphyr. Phthalocyanines*, vol. 14, no. 09, pp. 759–792, Sep. 2010.
[32] G. A. Crosby and J. N. Demas, “Measurement of photoluminescence quantum yields. Review,” *J. Phys. Chem.*, vol. 75, no. 8, pp. 991–1024, Apr. 1971.
[33] S. M. Borisov, G. Nuss, W. Haas, R. Saf, M. Schmuck, and I. Klimant, “New NIR-emitting complexes of platinum(II) and palladium(II) with fluorinated benzoporphyrins,” *J. Photochem. Photobiol. Chem.*, vol. 201, no. 2–3, pp. 128–135, Jan. 2009.
[34] A. Loudet, R. Bandichhor, L. Wu, and K. Burgess, “Functionalized BF2 Chelated Azadipyrromethene Dyes,” *Tetrahedron*, vol. 64, no. 17, pp. 3642–3654, Apr. 2008.
[35] S. M. Borisov and I. Klimant, “Efficient metallation in diphenylether – A convenient route to luminescent platinum(II) complexes,” *Dyes Pigments*, vol. 83, no. 3, pp. 312–316, Dezember 2009.
[36] K. Ichimura *et al.*, “Formation of tetrabenzoporphine skeleton by the reactions of phthalimide with zinc carbonates,” *Inorganica Chim. Acta*, vol. 186, no. 1, pp. 95–101, Aug. 1991.
[37] L. H. Hutter, B. J. Müller, K. Koren, S. M. Borisov, and I. Klimant, “Robust optical oxygen sensors based on polymer-bound NIR-emitting platinum(II)–benzoporphyrins,” *J. Mater. Chem. C*, vol. 2, no. 36, pp. 7589–7598, Aug. 2014.
[38] K. M. Kadish *et al.*, “Influence of Electronic and Structural Effects on the Oxidative Behavior of Nickel Porphyrins,” *Inorg. Chem.*, vol. 41, no. 25, pp. 6673–6687, Dezember 2002.
[39] S. M. Borisov, D. B. Papkovsky, G. V. Ponomarev, A. S. DeToma, R. Saf, and I. Klimant, “Photophysical properties of the new phosphorescent platinum(II) and palladium(II) complexes of benzoporphyrins and chlorins,” *J. Photochem. Photobiol. Chem.*, vol. 206, no. 1, pp. 87–92, Jul. 2009.
[40] K. R. Graham *et al.*, “Extended Conjugation Platinum(II) Porphyrins for use in Near-Infrared Emitting Organic Light Emitting Diodes,” *Chem. Mater.*, vol. 23, no. 24, pp. 5305–5312, Dezember 2011.
[41] C. Mongin, J. H. Golden, and F. N. Castellano, “Liquid PEG Polymers Containing Antioxidants: A Versatile Platform for Studying Oxygen-Sensitive Photochemical Processes,” *ACS Appl. Mater. Interfaces*, vol. 8, no. 36, pp. 24038–24048, Sep. 2016.
[42] K. Rurack and M. Spieles, “Fluorescence Quantum Yields of a Series of Red and Near-Infrared Dyes Emitting at 600−1000 nm,” *Anal. Chem.*, vol. 83, no. 4, pp. 1232–1242, Feb. 2011.
[43] X. Cai, B. Gao, X.-L. Li, Y. Cao, and S.-J. Su, “Singlet–Triplet Splitting Energy Management via Acceptor Substitution: Complanation Molecular Design for Deep-Blue Thermally Activated Delayed Fluorescence Emitters and Organic Light-Emitting Diodes Application,” *Adv. Funct. Mater.*, vol. 26, no. 44, pp. 8042–8052, Nov. 2016.
[44] X.-L. Chen *et al.*, “Highly efficient cuprous complexes with thermally activated delayed fluorescence and simplified solution process OLEDs using the ligand as host,” *J. Mater. Chem. C*, vol. 3, no. 6, pp. 1187–1195, Jan. 2015.
[45] Y. J. Cho, S. K. Jeon, B. D. Chin, E. Yu, and J. Y. Lee, “The Design of Dual Emitting Cores for Green Thermally Activated Delayed Fluorescent Materials,” *Angew. Chem. Int. Ed.*, vol. 54, no. 17, pp. 5201–5204, Apr. 2015.
[46] M. Kim, S. Kyu Jeon, S.-H. Hwang, S. Lee, E. Yu, and J. Yeob Lee, “Highly efficient and color tunable thermally activated delayed fluorescent emitters using a ‘twin emitter’ molecular design,” *Chem. Commun.*, vol. 52, no. 2, pp. 339–342, 2016.
[47] J. Lee, K. Shizu, H. Tanaka, H. Nomura, T. Yasuda, and C. Adachi, “Oxadiazole- and triazole-based highly-efficient thermally activated delayed fluorescence emitters for

organic light-emitting diodes," *J. Mater. Chem. C*, vol. 1, no. 30, pp. 4599–4604, Jul. 2013.
[48] S. Y. Lee, C. Adachi, and T. Yasuda, "High-Efficiency Blue Organic Light-Emitting Diodes Based on Thermally Activated Delayed Fluorescence from Phenoxaphosphine and Phenoxathiin Derivatives," *Adv. Mater.*, vol. 28, no. 23, pp. 4626–4631, Jun. 2016.
[49] X. Xiong *et al.*, "Thermally Activated Delayed Fluorescence of Fluorescein Derivative for Time-Resolved and Confocal Fluorescence Imaging," *J. Am. Chem. Soc.*, vol. 136, no. 27, pp. 9590–9597, Jul. 2014.
[50] H. Uoyama, K. Goushi, K. Shizu, H. Nomura, and C. Adachi, "Highly efficient organic light-emitting diodes from delayed fluorescence," *Nature*, vol. 492, no. 7428, pp. 234–238, Dezember 2012.
[51] P. Data, P. Pander, M. Okazaki, Y. Takeda, S. Minakata, and A. P. Monkman, "Dibenzo[a,j]phenazine-Cored Donor–Acceptor–Donor Compounds as Green-to-Red/NIR Thermally Activated Delayed Fluorescence Organic Light Emitters," *Angew. Chem. Int. Ed.*, vol. 55, no. 19, pp. 5739–5744, Mai 2016.
[52] J. Lee *et al.*, "Controlled emission colors and singlet–triplet energy gaps of dihydrophenazine-based thermally activated delayed fluorescence emitters," *J. Mater. Chem. C*, vol. 3, no. 10, pp. 2175–2181, Feb. 2015.
[53] S. Wang, X. Yan, Z. Cheng, H. Zhang, Y. Liu, and Y. Wang, "Highly Efficient Near-Infrared Delayed Fluorescence Organic Light Emitting Diodes Using a Phenanthrene-Based Charge-Transfer Compound," *Angew. Chem. Int. Ed.*, vol. 54, no. 44, pp. 13068–13072, Oktober 2015.
[54] Q. Zhang *et al.*, "Anthraquinone-Based Intramolecular Charge-Transfer Compounds: Computational Molecular Design, Thermally Activated Delayed Fluorescence, and Highly Efficient Red Electroluminescence," *J. Am. Chem. Soc.*, vol. 136, no. 52, pp. 18070–18081, Dezember 2014.
[55] C. A. Parker and C. G. Hatchard, "Triplet-singlet emission in fluid solutions. Phosphorescence of eosin," *Trans. Faraday Soc.*, vol. 57, no. 0, pp. 1894–1904, Jan. 1961.
[56] J. Mack, Y. Asano, N. Kobayashi, and M. J. Stillman, "Application of MCD spectroscopy and TD-DFT to a highly non-planar porphyrinoid ring system. New insights on red-shifted porphyrinoid spectral bands," *J. Am. Chem. Soc.*, vol. 127, no. 50, pp. 17697–17711, Dec. 2005.
[57] E. R. Carraway, J. N. Demas, B. A. DeGraff, and J. R. Bacon, "Photophysics and photochemistry of oxygen sensors based on luminescent transition-metal complexes," *Anal. Chem.*, vol. 63, no. 4, pp. 337–342, Feb. 1991.
[58] B. J. Müller, T. Burger, S. M. Borisov, and I. Klimant, "High performance optical trace oxygen sensors based on NIR-emitting benzoporphyrins covalently coupled to silicone matrixes," *Sens. Actuators B Chem.*, vol. 216, pp. 527–534, Sep. 2015.
[59] A. M. A. El Wafa, S. Okada, and H. Nakanishi, "Poling and its relaxation studies of polycarbonate and poly(styrene-co-acrylonitrile) doped by a nonlinear optical chromophore," *Dyes Pigments*, vol. 69, no. 3, pp. 239–244, Jan. 2006.
[60] B. Ellis and R. Smith, *Polymers: A Property Database, Second Edition*. CRC Press, 2008.
[61] R. R. Islangulov, J. Lott, C. Weder, and F. N. Castellano, "Noncoherent low-power upconversion in solid polymer films," *J. Am. Chem. Soc.*, vol. 129, no. 42, pp. 12652–12653, Oct. 2007.
[62] T. N. Singh-Rachford and F. N. Castellano, "Pd(II) phthalocyanine-sensitized triplet-triplet annihilation from rubrene," *J. Phys. Chem. A*, vol. 112, no. 16, pp. 3550–3556, Apr. 2008.

[63] T. N. Singh-Rachford, J. Lott, C. Weder, and F. N. Castellano, “Influence of temperature on low-power upconversion in rubbery polymer blends,” *J. Am. Chem. Soc.*, vol. 131, no. 33, pp. 12007–12014, Aug. 2009.
[64] Y. Y. Cheng *et al.*, “On the efficiency limit of triplet–triplet annihilation for photochemical upconversion,” *Phys. Chem. Chem. Phys.*, vol. 12, no. 1, pp. 66–71, Dec. 2009.
[65] A. J. Svagan, D. Busko, Y. Avlasevich, G. Glasser, S. Baluschev, and K. Landfester, “Photon Energy Upconverting Nanopaper: A Bioinspired Oxygen Protection Strategy,” *ACS Nano*, vol. 8, no. 8, pp. 8198–8207, 2014.